ABSTRACT

CARROLL, PAUL MICHAEL. An Evaluation of Two Cross-shore Numerical Models in Predicting Subaerial Beach Morphology. (Under the direction of Dr. John S. Fisher.)

Numerical modeling in the nearshore region has become an important tool in both planning and design for coastal engineers. In recent decades, the complexity of these models has increased as our knowledge of existing processes has matured. However, gaps still remain between what we as engineers understand about the nearshore environment and what actually exists. Due to these uncertainties, modelers have taken different approaches to simulate sediment transport.

The objective of this thesis is to evaluate the ability of two cross-shore numerical models, SBEACH and COSMOS, in their ability to predict subaerial beach profile change resulting from storm events. The predicted profiles from each model were compared to actual measured post-storm profiles. Quantitative comparison of results from both models was preformed using BMAP (Beach Morphology Analysis Package). A rating of good, fair, or poor was assigned to the models based on how closely each predicted the measured subaerial profile change. The waterline recession was also analyzed and a rating of reasonable or unreasonable was assigned to each model based on its predicted value.

The fundamental difference between the two models is in regards to sediment transport. The SBEACH model predicts sediment transport rates as a function of wave energy dissipation. The COSMOS model utilizes the energetics approach where sediment transport is dependent on mean velocity currents in both the bed and the suspended boundary layers. The results presented within this report show that

SBEACH performed equally as well or better in each case. The COSMOS model consistently over predicted erosion on the beach face and recession of the waterline. For the study sites where data was collected for this research, SBEACH is the recommended model by the author.

An Evaluation of Two Cross-shore Numerical Models in Predicting Subaerial Beach Morphology

By

Paul Michael Carroll

A thesis submitted to the Graduate Faculty of
North Carolina State University
In partial fulfillment of the
Requirements for the Degree of
Master of Science

CIVIL ENGINEERING

Raleigh

2004

APPROVED BY:

_____ _____

_____
Chair of Advisory Committee

PERSONAL BIOGRAPHY

Paul Michael Carroll was born in Arlington, Virginia on August 4, 1979. He is the third child born out of four to Michael and Mary Carroll. In 1998 Paul graduated from George C. Marshall High School and went on to study Civil Engineering at the Virginia Military Institute (VMI) in Lexington, Virginia. After graduating from VMI Paul went on to pursue a Masters of Science in civil Engineering from North Carolina State University.

ACKNOWLEDGEMENTS

The author would like to express his sincere gratitude to Dr. John S. Fisher and Dr. Margery F. Overton for their guidance during the course of this academic endeavor. Special thanks also go to Mohammad Dibajnia and Robert Nairn of Baird and Associates, Kent Hathaway of the FRF, and Christopher Mack of the Army Corps of Engineers for their help along the way. Robert Nairn, one of the authors of the COSMOS model, was kind enough to provide a copy of the model. Mohammad was the connection which enabled the acquisition of the COSMOS model, without which this project would not have materialized. He was also very helpful in answering questions and checking some of the author's work early on in the process. Several times the author contacted Kent Hathaway with questions about the data provided by the FRF and every time Kent was willing to spend some of his time discussing the data involved. Christopher provided the BMAP program so that quantitative analysis could be performed. And most importantly the author would like to thank the friends who were there, they know who they are.

TABLE OF CONTENTS

LIST OF TABLES

LIST OF FIGURES

1. INTRODUCTION

The dynamic nature of nearshore systems in coastal regions poses a difficult challenge to coastal engineers. Nearshore processes are influenced by the constantly changing forces of winds and waves which have three dimensional effects that are difficult to predict in time and space. Surf zone hydrodynamics are very complex and are not well understood at the present time. Over the past few decades numerical modeling of the coastal region has become an important tool. Modelers have made various assumptions to simplify the contributing factors in order to attain a generally accurate prediction of change. The complex nature of the coastal environment has led some modelers to rely more heavily on empirical evidence rather than the pure physics associated with existing processes.

Creating a model of a system can be a powerful tool to study and understand certain processes. Two types of models are physical models and numerical models. An example of a physical model in coastal engineering is a wave tank, where waves are generated and applied to a beach profile to produce a change. The usage of numerical models for the nearshore region has become increasing popular over the last couple decades as the capabilities personal computers have improved. Many numerical models for the littoral zone have been developed by various researchers to predict the 2-dimensional change of a beach profile resulting from varying water levels and wave heights. Effects of wind can also be incorporated in certain models but are often considered to have insignificant effects when compared to wave action and are therefore left out of the analysis. More recently models have been expanded to incorporate three dimensional effects.

2. OBJECTIVE

The objective of this research was to compare the ability of two cross-shore numerical models to replicate measured subaerial beach profile change after a storm event. Data was collected at two North Carolina Study sites, Buxton and Duck, which measured beach profile change as a result of two storm events, Hurricane Dennis and Hurricane Isabel. An important feature common to the beaches in both of the selected study sites are dunes. Dunes form a protective barrier from storms; they help to protect homes, roads, and other structures built too close to the shoreline from flooding and other damages. The storage of sand within the dune is often eroded by large waves during storm events and moved offshore to form a bar.

Initially the present study focused primarily on the dunes themselves. However, in most of the cases presented here, the post-storm profiles did not show enough measurable change within the dune alone to make quantitative comparisons. Therefore the region looked at was expanded to include the beach face. Recession of the waterline was also a feature considered. The waterline, in the examples provided in this report, is identified as the location where the profile intersects the 0 meter contour. The waterline is commonly used in the determination of set-back distances for development of ocean front property.

3. CROSS-SHORE TRANSPORT MODELS

The ability to model cross-shore transport is of vital importance to coastal communities as cross-shore transport becomes the dominant mechanism during storm events. Because of this, in areas such as the Outer Banks of North Carolina, predicting the impact of a storm event aids in determining roadway vulnerability, planning of set-back distances, and setting regulations to reduce potential damages from such events.

Sediment transport caused by the stirring of sediment and current action in the nearshore region results in beach profile change. Numerous theories have been developed to describe how sediment is stirred and then transported in an aqueous environment. Various modelers have adopted differing transport theories. One of the more established theories was developed by Ralph Bagnold who used experiments in open channel flow to develop general relationships where the rate of transport is a function of the flow strength. He describes transport occurring in two layers: the bed layer and suspended layer. The work of Bagnold has been expanded upon in more recent numerical models such as Bowen's 1980 model, Bailard's 1981 model, and the COSMOS model, Nairn and Southgate (1993).

For this work the idea was to compare two cross-shore transport models using common datasets. COSMOS and SBEACH were selected because both are well known and were both easily obtained. SBEACH was developed by the United States Army Corps of Engineers, (USACE) authored by Larson and Kraus (1989), Larson *et al.* (1990), Rosati *et al.* (1993), Wise *et al.* (1996). COSMOS is a privately owned model developed by HR Wallingford (United Kingdom), authored by Nairn and

Southgate (1993), Southgate and Nairn (1993). The COSMOS model was made available for use in this work courtesy of Dr. Robert Nairn, and the SBEACH model was made available courtesy of Dr. Margery Overton and Dr. John Fisher.

SBEACH is widely used by the USACE and common applications of the model are for beach fill design and beach erosion prediction resulting from short term events. The model was developed with significant reliance on empirical data derived from large wave tank (LWT) tests. The authors argue that because much is still unknown about the dynamics of the nearshore region, empirical evidence must be used. Therefore empirical relationships were derived between wave conditions and the development and movement of major profile features such as berms and bars. A series of four reports describing the model has been produced by the Army Corps of Engineers. The first report contains a review of laboratory and field studies, derivation of sediment transport relationships, the profile change model, the wave model, and results of field validation tests (Larson and Kraus, 1989). Further field testing is provided in the second report (Larson *et al.*, 1990). The third report serves as a user's manual (Rosati *et al.,* 1993). Report four describes model revisions which improved the random wave component (Wise *et al.,* 1996).

The COSMOS model was developed by Nairn and Southgate (1993), and Southgate and Nairn (1993). It uses the energetics approach to sediment transport, first developed by Bagnold. Bagnold assumed that sediment transport was a function of energy dissipation per unit bed area, meaning transport of sediment occurs as a result of turbulence in the water column, and it occurs in either bedload or suspended load. Bedload defined by Bailard (1981) is sediment moving within the bed boundary

layer. He defines suspended load as transport above the bottom boundary layer. A description of this model and an outline of the theory used are provided in two papers written by Howard Southgate and Robert Nairn. The first paper describes the wave and current model (Southgate and Nairn, 1993) while the second paper focuses on sediment transport and profile change (Nairn and Southgate, 1993).

4. THE SBEACH MODEL

This chapter is intended to highlight the purpose and theoretical basis of the SBEACH model. For a complete description of the model the reader is referred to reports 1- 4 of the SBEACH literature (Larson and Kraus, 1989, Larson and Kraus, 1990, Rosati *et. al.*, 1993, and Wise *et. al.*, 1996).

The primary application of the SBEACH model is to predict cross-shore beach morphology, on a scale of feet or meters, resulting from storm events on a time scale of hours or days. A fundamental assumption made by the authors of SBEACH is that within the short time frame of a storm event the primary transport mode is normal to the shore, and thus longshore transport is assumed to maintain continuity. Continuity infers that whatever sediment enters a particular profile from the up-drift direction, the same amount exits the profile in the down-drift direction. This assumption is made by both SBEACH and COSMOS and allows the problem to be reduced to two dimensions. In the field this assumption is not always valid. For instance where there is a feature that interrupts the natural longshore current, conservation of mass is not upheld. Features such as groins, jetties, inlets, breakwaters, etc. disrupt the natural current parallel to the beach, either increasing or decreasing the sediment concentration in the alongshore stream. Thus the sediment concentration in to a particular profile is not the sediment concentration exiting the profile. Because of this assumption these models should only be applied to coastal sections that are free of any disrupting features and that contain more or less uniform characteristics.

Sediment transport equations used by SBEACH, for the most part, are based heavily on empirical data derived from wave tank tests. It is an empirical model, as opposed to the COSMOS model which has a more theoretical sediment transport approach dealing with velocity vectors for each layer of flow. The majority of transport in SBEACH is assumed to occur within the surf zone and is assumed to be driven mainly by the dissipation of energy from breaking waves.

In both models, wave and water level conditions determine beach profile change. The authors of SBEACH used relationships between wave and profile parameters observed in large wave tank experiments (CE and CRIEPI data sets) to develop transport rate equations for four distinct transport zones. The model was then verified using field data from various sites. The first LWT data set, CE, was gathered from experiments performed by the US Army Corps of Engineers (USACE) in the years 1956-1957, and 1962. The second data set was obtained from experiments performed at the Central Research Institute of Electric Power Industry (CRIEPI) in Japan. All experiments were conducted using waves of constant height and period.

4.1 SBEACH Model Theory

Turbulence within the water column creates and maintains a suspended concentration of sediment, and current velocities move the sediment. The amount of turbulence is related to the parameters of the breaking waves, implying that transport inside the surf zone is governed by different hydrodynamics than outside of the surf zone.

Based on observations from LWT tests, Larson and Kraus (1989) identified four separate transport regions, characterized by different wave climates for

monochromatic waves, and three regions for random waves. As stated above, SBEACH assumes sediment transport is mainly caused by wave energy dissipation. Profile change is calculated using the sediment transport relationships and conservation of mass, equation 1. Where the sediment transport rate, q, in the cross-shore direction, x, is related to the wave height h, at time t.

$$\frac{dq}{dx} = \frac{dh}{dt} \qquad (1)$$

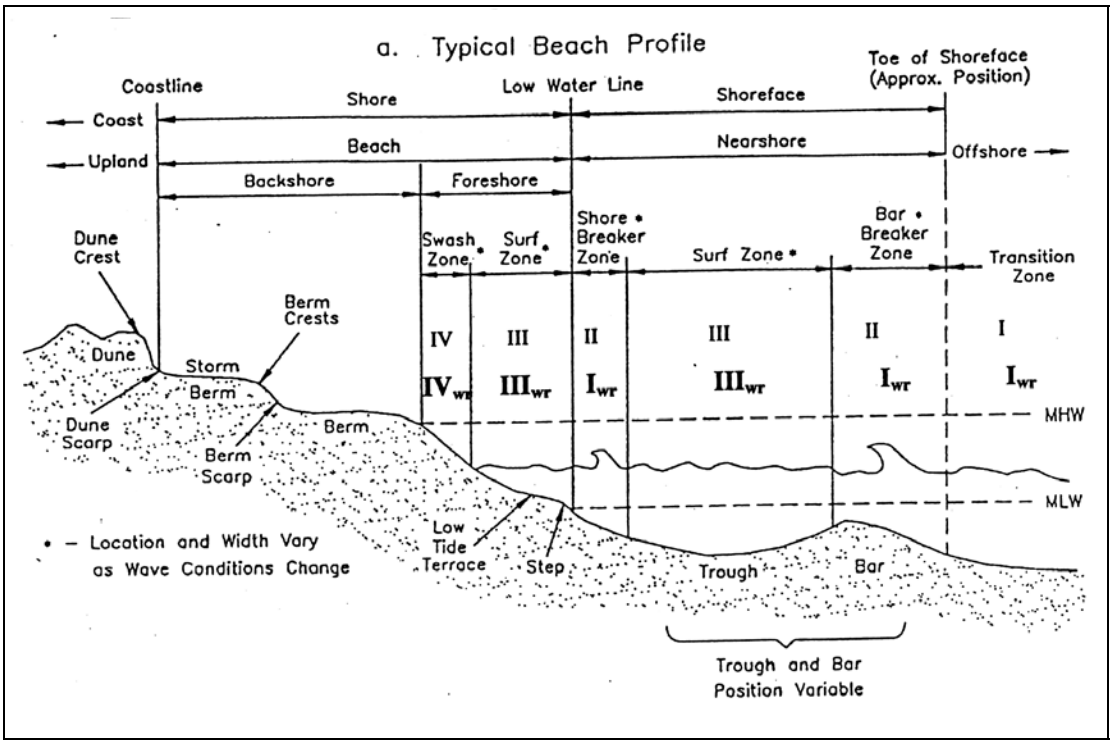

Figure 4.1. Typical Beach Profile originally created by USACE then altered to show roman numerals by Miller (1998). Plain text Roman numeral are for monochromatic waves, bold text Roman numerals are for random waves.

4.1.1 Wave Model

SBEACH is capable of predicting profile evolution resulting from either monochromatic waves or random waves. Monochromatic waves, waves having the same heights and periods, break at a common point corresponding to a breaking

depth. Random waves are waves which have varying heights and periods, causing them to break at different locations along the profile. A benefit of modeling the effects of monochromatic waves is that the profile features that result from a particular wave climate can be more readily seen. However, a random wave environment is one that better represents the activities in the field.

Since its initial development, the wave model in SBEACH has been improved. In particular how it calculates wave characteristics for random waves has been updated with the help of Wise *et al*. (1996). With this revision, the number of transport zones was reduced to three. These are labeled with bold roman numerals in Figure 4.1. A detailed description of the random wave model is provided in Wise *et al*. (1996).

The wave model provides input values used in the transport model which is described later in this chapter. Linear wave theory is applied for Zone I, from the break point seaward to the depth of closure, to calculate wave parameters. A generalized version of the Dally *et al*. (1985) model is applied in the surf zone, zone III. The user provides information about waves specified from a point off-shore. When simulating a storm this information typically includes a time series of wave heights and periods, water levels, and a value describing the incident wave angle. The model calculates wave heights beginning with the most seaward cell using either conservation of energy flux when waves arrive normal to bathymetric contours, or Snell's law when waves arrive at an angle and refraction has to be considered. Sediment transport within the zones of non-breaking waves is calculated based on

empirical relationships derived from wave tank experiments, and energy dissipation does not play a role (Zones I, II, and IV).

The energy dissipation from waves that is available for sediment transport is that which is in excess of the equilibrium energy dissipation rate, which is a function of both wave conditions and beach geometry. The energy dissipation, D, for profile regions shoreward of the breakpoint is found with equation 2.

$$D = \frac{\kappa}{d^2}\left(F - F_{st}\right) \qquad (2)$$

where

F_{st} = stable energy flux

F = energy flux

κ = empirical wave decay coefficient

d = total water depth

The stable energy dissipation rate is calculated with equation 3. It is a function of water density, mean sediment size, and wave steepness.

$$D_{eq} = \left(\frac{5}{24}\right)\rho g^{\left(\frac{3}{2}\right)}\gamma^2 A^{\left(\frac{3}{2}\right)} \qquad (3)$$

where

ρ = water density

g = acceleration due to gravity

γ = ratio between wave height and water depth

A = term related to mean sediment size

Transport rates decay with time as a profile approaches its equilibrium shape. Investigations using monochromatic waves and constant water levels show that transport rates between the initial and final time steps of a run can vary by an order of magnitude. The literature describes how transport rates were obtained by finding net volume changes between consecutive profiles in time and applying conservation of mass Larson *et al.* (1990). In general, transport rates are higher the further away a profile is from its equilibrium shape according to the current wave conditions.

The energy flux is solved using equation 4.

$$F = \left(\frac{1}{8}\right)\rho g H^2 \sqrt{gh} \qquad (4)$$

where

H = wave height

The stable energy flux is a value that is related to the wave conditions and does not vary for a specific wave environment. When the energy flux is equal to the stable energy flux, it is assumed that no significant amount of sediment is transported.

$$F_{st} = \left(\frac{1}{8}\right)\rho g (\Gamma d)^2 C_g \qquad (5)$$

where

Γ = empirical stable wave height coefficient, equal to 0.40

C_g = wave group speed

Equation 5 can be re-written as equation 6, here showing the stable energy flux as a function of a stable wave height.

$$F_{st} = \left(\frac{1}{8}\right)\rho g (H_{st})^2 C_g \qquad (6)$$

Wave breaking takes place once a critical ratio between wave height and water depth is reached. This ratio is labeled the breaker index, and experiments show that this value increases with a steeper slope and decreases with an increase in wave steepness (Larson and Kruas, 1989).

The breaker index is determined by equation 7.

$$\gamma = 1.14\zeta^{0.21} \qquad (7)$$

where

ζ = the surf similarity parameter

The surf similarity parameter is a term which considers beach slope and is calculated with equation 8.

$$\zeta = \tan\beta\left(\frac{H_o}{L_o}\right)^{-0.5} \qquad (8)$$

where

$\tan\beta$ = the local slope of beach seaward of break point

H_o = deep water wave height

L_o = deep water wave length

After the wave height is determined across shore, energy dissipation can be calculated using equation 2. Outside the surf zone, κ is considered to have a value of zero, thus transport resulting from energy dissipation is not considered. A minimum energy dissipation rate threshold exists within the zone of breaking waves. If the existing dissipation rate is not greater than the equilibrium dissipation rate minus a term that takes profile steepness into account, the net transport in that zone is zero Larson and Kraus (1989).

4.1.2 Random Waves

In the random wave model, beyond the surf zone a field of waves is expected to have a variation in wave heights that follow the Rayleigh distribution. For this case the Rayleigh distribution is a statistical description of the probability that a wave will have a deepwater wave height that is greater than a certain value (Dean and Dalrymple, 1984). Shoreward of the point of wave breaking a generalized version of the Dally *et al*. (1985) model is used to describe wave height decay across the surf zone. Beginning in deepwater a single representative wave composed of components from a large number of waves is transformed across the profile. As this single wave is transformed the fraction of broken, unbroken, and reformed waves are determined. The method used in SBEACH for modeling the decay of random waves in the surf zone is described in Larson (1995). This method is preferred over the Battjes and Janssen (1978) model because no assumption about the probability-density function (pdf) for waves in the surf zone is needed.

The transport relationships, as mentioned, were revised for the newer random wave model. In zones of unbroken waves the transport rates for the pre-breaking zone and the swash zone become equations 9 and 11, respectively. Equation 10 becomes the revised relationship for sediment transport in a random wave field under broken waves where α represents the fraction of broken waves.

$$q = \frac{1}{N}\sum_{i=1}^{n} q_{bi} e^{-\lambda_i (x - x_{bi})} \qquad \text{(Region I)} \qquad (9)$$

$$q = \left\{ K\xi \left(D - \alpha \left(D_{eq} - \frac{\varepsilon}{K}\frac{dh}{dx} \right) \right) \right\} \quad \text{or} \qquad \text{(Region III)} \qquad (10)$$

$$q = \{0\} \qquad \text{if} \quad \mathrm{D} \le \left(D_{eq} - \frac{\varepsilon}{\kappa} \frac{dh}{dx} \right)$$

$$q = q_s \left(\frac{x - x_r}{x_s - x_r} \right)^{3/2} \qquad \text{(Region IV)} \quad (11)$$

where

q = cross shore transport rate

D = energy dissipation rate

ε = transport rate coefficient for slope-dependent term

K = empirical transport rate coefficient

h = still water depth

x_r = location of run-up limit

x_s = shoreward location of surf zone

q_s = cross shore transport rate at the shoreward boundary of the surf zone

ξ = transport function

N = the total number of waves

The notation, *bi*, denotes the break point of wave *i*. The authors assumed that the difference between the spatial decay coefficient of the pre-breaking zone and the transition zone is negligible, and so the breaker transition zone (zone II) is not included in a random wave environment. For random waves, equation 11 applies for the region seaward of the plunge point.

Zone I extends from the plunge point seaward to the depth of closure for random waves. The depth of closure is typically defined as the seaward point where no measurable depth variation takes place between consecutive surveys. The

sediment transport into or out of this region is proportional to the transport rate at the seaward end of the breaking zone and then decays at an exponential rate with distance seaward. The spatial decay coefficient, λ_1, is an empirical value related to the mean sediment size and breaking wave height.

$$\lambda_1 = m_* \left(\frac{D_{50}}{H_b} \right)^{0.47} \qquad (12)$$

In the random wave model the effects of each individual broken wave are considered so that a net transport rate can be found. This includes waves that have not broken, waves that have reformed, and waves that have stopped breaking. Equation 13 effectively expresses how the average transport rate is computed using each individual wave.

$$q = \frac{1}{N} \sum_{i=1}^{m} q_i \qquad (13)$$

where

N = the total number of waves

m = the number of broken waves

q_i = the transport rate for wave *i* at x.

Zone III is of primary interest because it is the zone of fully broken waves. It extends from the plunge point shoreward to the beginning of the swash zone. SBEACH assumes that the driving force behind sediment transport, and subsequently profile change, is breaking waves. Sediment transport within this zone is a function of the wave energy dissipation per unit volume of water. The wave energy is related to the wave height which is calculated using the breaker decay model of Dally *et al.* (1985) for random waves. Note that equation 10 includes a threshold value below

which the transport rate is equal to zero. The equation states that if the energy dissipation rate, reduced by a term which takes into account the local profile slope, is not greater than the equilibrium dissipation rate, the transport rate is equal to zero.

5. THE COSMOS MODEL

The approach taken in the COSMOS model is one based on the physical processes that exist in the nearshore region. Unlike SBEACH, COSMOS attempts to model both waves and currents. It uses the energetics approach to describe sediment transport. Based on concepts first introduced by Bagnold the idea behind the energetics approach is that some fraction of the total fluid energy is expended maintaining the sediment in suspension (Southgate and Nairn, 1993). The COSMOS wave model incorporates the influences of both waves and wave induced longshore and cross-shore currents to predict beach profile change. Sediment is transported either as bed load or suspended load as a function of mean time averaged velocity vectors.

After transport rates are calculated, profile morphology is determined through the continuity equation. COSMOS has been developed to model short to medium term events, durations ranging from days to months, making it effective both as a planning tool and an indicator of storm impact. A point emphasized in the literature, Nairn and Southgate (1993), is that the use of free variables or calibration parameters is kept to a minimum. Instead improvement should be made by better representing the actual processes or inclusion of additional processes such as the effects of tidal currents or infragravity waves.

5.1 COSMOS Model Theory

The following section outlines the theoretical basis for the energetics approach which was first developed from experiments with open channel flow. In bed load transport, the work done per unit time by the fluid to keep particles moving is the

tangential thrust needed to overcome friction, multiplied by the mean speed at which the grains are traveling (Nairn and Southgate, 1993). Equation 16 describes the power used to maintain bedload. In this formulation, i_b is the immersed weight transport rate, ϕ is the angle of internal friction, and $\tan\beta$ is the bed slope.

$$\text{Fluid power expended} = i_b\left(\tan\phi - \tan\beta\right) \tag{16}$$

Since only some fraction of the total power is available for the advection of sediment, equation 17, for the immersed weight transport rate, includes an efficiency factor, ε_b.

$$i_b = \omega\frac{\varepsilon_b}{\left(\tan\phi - \tan\beta\right)} \tag{17}$$

The ω term in the above expression is the dissipated fluid power which is related to boundary shear stress and the near bed velocity in equation 18. The c_f term in equation 18 is a friction coefficient.

$$\omega = c_f \rho u_t^3 \tag{18}$$

The suspended weight transport rate has a similar derivation. The work done per unit time to transport grains in the suspended layer is a function of both the normal stress and the fall velocity. Equation 19 describes the power used in transporting a suspended load. This formula includes a term for fall velocity, w.

$$\text{Fluid Power expended} = i_s\left(\frac{w}{u_s} - \tan\beta\right) \tag{19}$$

The suspended weight transport rate was originally described as illustrated by equation 20.

$$i_s = \omega \frac{\varepsilon_s}{\left(\frac{w}{U_s} - \tan\beta \right)} \qquad (20)$$

Equation 21 describes the total submerged weight transport rate.

$$i = i_b + i_s = K\omega = \left(\frac{\varepsilon_b}{\tan\varphi - \tan\beta} + \frac{\varepsilon_s}{w/U_s - \tan\beta} \right)\omega \qquad (21)$$

ε_b = efficiency factor for bed load transport, equal to 0.10

ε_s = efficiency factor for suspended load transport, equal to 0.020

Nairn and Southgate (1993) describe the development of the energetics approach through the work of various authors. The original formulation was for the purpose of modeling sediment transport in streams, later it was applied to the nearshore environment to model cross-shore sediment transport.

5.2 COSMOS Wave Model

In the COSMOS wave model there is full interaction between waves and currents as each influences the other. Waves influence currents through a friction factor and by the generation of longshore currents during breaking, and currents affect waves through refraction and wave friction (Nairn and Southgate, 1993). Longshore currents resulting from the influence of tides can also be accounted for through superposition but will not be considered here. The model takes into account the following wave processes; shoaling, refraction, seabed friction and wave breaking.

COSMOS uses a parametric wave approach where orbital velocities, mean currents and sediment transport rates are calculated based on a single wave height and peak period. The single wave is propagated through each grid point moving

shoreward. This approach is different than the SBEACH single wave approach in that it makes an assumption about the distribution of waves in within the surf zone. This model uses a Raleigh distribution of wave heights truncated at the breaker height to simulate the breaking of random waves in the surf zone (Southgate, 1989). The user can specify a single root mean square (rms) wave height, a peak wave period, and mean direction to represent a wave spectrum. In this study multiple wave conditions downloaded from the FRF website were used to represent selected storm events. These measurements are assumed to be taken at the seaward most point on the profile which should always be located outside the surf zone. The wave action equation, equation 23, developed by Christoffersen and Jonsson (Nairn and Southgate, 1993, is used to calculate dynamic wave quantities such as the wave height and energy. Wave energy is derived from dissipation from both breaking waves and bottom friction.

$$\frac{d}{dy}\left(\frac{EC_{ga}\cos\mu}{\omega_r}\right) = -\frac{\left(D_f - D_b\right)}{\omega_r} \qquad (23)$$

where

y = coordinate on the axis normal to the shore

E = wave energy density

C_{ga} = absolute wave group velocity

μ = wave ray angle

ω_r = relative wave angular frequency

H = wave height

D_f = wave energy flux dissipation by bottom friction

D_b = wave energy flux dissipation by wave breaking

The wave energy density is related to wave height by equation 24.

$$E = \frac{1}{8}\rho g H^2 \tag{24}$$

Dissipation terms for bottom friction and wave breaking that are found in equation 23, are solved using equations 25 and 27.

$$D_f = \rho C_{fw} u_m^3 \tag{25}$$

where

C_{fw} = the wave friction factor

u_m = peak wave orbital velocity at the seabed

$$u_m = \frac{H\omega_r}{2\sinh(kh)} \tag{26}$$

$$D_b = \frac{\lambda\rho g^{\frac{3}{2}} k H_{rms}^3 f(Q_b)}{8\pi h^{\frac{1}{2}}} \tag{27}$$

COSMOS uses the model presented by Batties and Janssen (1978) to simulate the rate of energy dissipation in the surf zone for random waves. Within this process, the ratio of breaker height to depth (H_b/h) must be determined, the fraction of broken and breaking waves, Q_b, must be solved for using equation 29, and the energy dissipation rate, D_b, must be calculated. The method assumes a Rayleigh distribution of wave heights around a single rms wave height to determine the local fraction of waves that are breaking (Southgate and Nairn, 1993).

5.3 Currents

As mentioned previously, the wave model includes the interaction of waves and currents. Both cross-shore and longshore currents are accounted for in the model. During strong wave conditions, the undertow current is believed to be an important mechanism in profile erosion. The undertow is a steady current existing near the seabed in the offshore direction. COSMOS models the undertow current following the theory of De Vriend and Stive (1987) (Southgate and Nairn, 1993), who used a three layer approach. Longshore currents are calculated from the wave energy dissipation rate. Though they are accounted for in the model for their interaction with waves, none of the simulations performed in this study included sediment transport in the alongshore direction.

5.4 Transition Zone

When a wave breaks the total amount of energy from that wave to be dissipated is not realized until the wave propagates some distance past the break point to a point often referred to as the plunge point. The zone between the break point and the plunge point is referred to as the transition zone, labeled region II for monochromatic waves on Figure 4.1. Research conducted by the authors of COSMOS found that including a transition zone during model simulations improves results. The authors of SBEACH found that for the case of random waves, the effect of this zone was less apparent and is not accounted for. Comparisons between COSMOS results performed during the course of this study revealed no change when the transition zone was included, thus a transition zone was not used for COSMOS simulations.

5.5 Onshore Transport

The COSMOS model has been shown to be capable of predicting onshore transport. Onshore transport is driven mainly by waves which have asymmetric surface profiles, showing a forward pitch at the crest (Bosboom, 2000). Provided in Nairn and Southgate (1993) are a few examples of where measured data from field or large scale experiments compared well with predicted values from COSMOS. An experiment using a large wave flume showed that measured sediment transport rates matched well with predicted rates. A beach recovery event documented at the FRF site was used to test the model's predictive abilities under field conditions, again results from the model compared well to the measured profile change. The ability to model onshore transport by SBEACH has not yet been verified according to Wise *et al.* (1996).

6. STUDY AREAS

6.1 Buxton

Buxton, North Carolina is located on Hatteras Island, northeast of Hatteras Inlet. With Pamlico Sound on the back side of the island, it is part of a barrier island system that makes up the Outer Banks. The section of Buxton where profiles were gathered is a narrow strip of land, less than 300 meters wide with a single row of dunes. Just landward of the dune line is North Carolina Highway 12 (NC12), a vital corridor for residents of Cape Hatteras.

6.2 Duck

The Field Research Facility, FRF, located in Duck, North Carolina, is operated by the US Army Corps of Engineers for the purpose of coastal research. This section of the Outer Banks is about 700 meters wide. Behind the beach at the FRF is a dune field. Despite being located in a region often battered by seasonal storm events, little change to the subaerial beach is ever seen. A commonly suggested reason for this anomaly is an abundance of coarse sediment found on the foreshore (Larson and Kraus, 1989). This site was selected because of the quality profile and wave and water level data that is collected and publicly available through the FRF website.

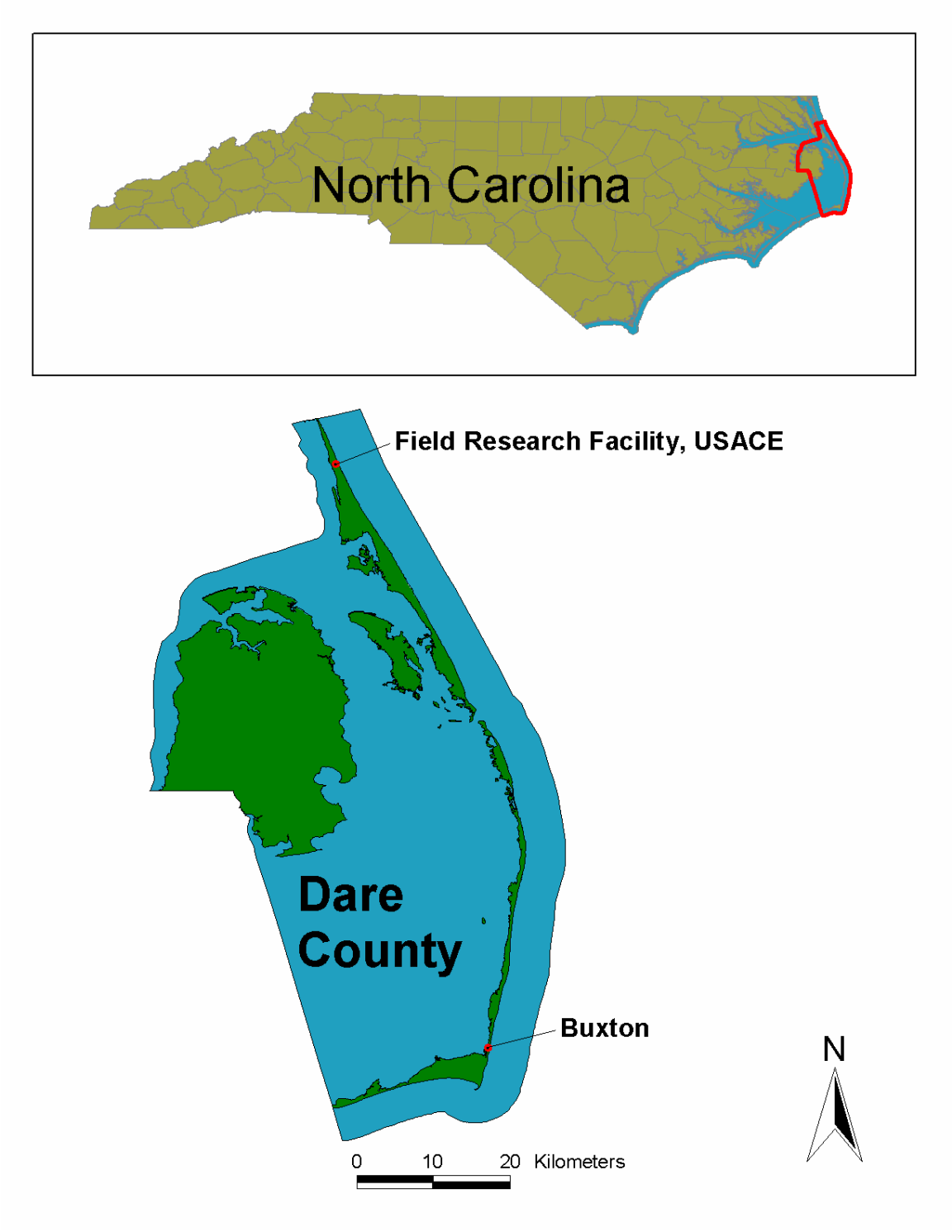

Figure 6.1. Location Map.

7. STORM EVENTS

The FRF website (http://www.frf.usace.army.mil/) was the source used for wave and water level information during both Hurricane Dennis and Hurricane Isabel. In order to simulate a storm event in either SBEACH or COSMOS a record of wave heights, wave periods, and water levels must be provided by the user. This storm data is ideal for being applied to the FRF profiles and is the closest source of wave and water level information to the Buxton site (approximately 80 kilometers to the north of Buxton) to the knowledge of the author.

7.1 Hurricane Dennis

Figure 7.1 shows the data used to represent Hurricane Dennis. Hurricane Dennis originated in the Bahamas on August 24th, 1999. By August 26th, the storm had reached hurricane strength. As Dennis moved up the east coast and approached the Carolinas it began to weaken. On August 30th, the storm was nearing the North Carolina coast, but then changed directions and moved further out to sea on a northeasterly track. It then changed course again towards the south. Though it was out at sea, the wind field from Dennis stretched 320 kilometers in every direction from its center battering the coast with strong winds and waves for days (Barnes, 2001). On the first of September, Dennis was downgraded to a tropical storm. During the two days that followed, Dennis began to re-intensify and head once more toward the North Carolina coast. Tropical storm Dennis made landfall on the afternoon of September 4th along Cape Lookout National Shoreline.

The unusually long duration of this storm resulted in the worst coastal erosion the Outer Banks had seen in years (Barnes, 2001). Dennis created two peak storm

tides of 1.75 and 1.1 m respectively. The first occurred as the storm moved past the coast on August 30th, and the second occurred when Dennis made landfall on September 4th. Storm tide is the combination of the resulting surge in water level due to the storm and the normal astronomical tide.

7.2 Hurricane Isabel

Figure 7.2 shows the data used to represent Hurricane Isabel. Hurricane Isabel developed in early September 2003 as a tropical storm headed west toward the Caribbean. On September 12th, it had reached its maximum strength as a category 5 hurricane. Sweeping across the mid-Atlantic, Isabel began to turn northwest on September 14th, and headed straight for the Outer Banks. Six days after reaching her maximum strength, Isabel made landfall on September 18th near Cedar Island, NC. At that time Isabel was a category 2 hurricane recording sustained winds near 160 kph (National Weather Service website, 2004). After making landfall the storm continued to move up through eastern North Carolina and Virginia. Isabel caused coastal erosion along the Outer Banks and in Virginia as well as widespread power outages and several deaths.

7.3 Wave and Water Level Data

Water level is recorded every 6 minutes by a National Oceanic and Atmospheric Administration (NOAA) gauge located at the seaward end of the FRF pier. Wave data is derived from gauge 3111, which is actually a collection of a number of different instruments from which an energy-based statistical value for wave height, equal to the significant wave height, as well as a peak wave period is produced (FRF website, 2003). Wave angle relative to true north is also provided by

gauge 3111. The collection period is about 2 hours and 51 minutes. Water levels are measured from the 1929 National Geodetic Vertical Datum (NGVD).

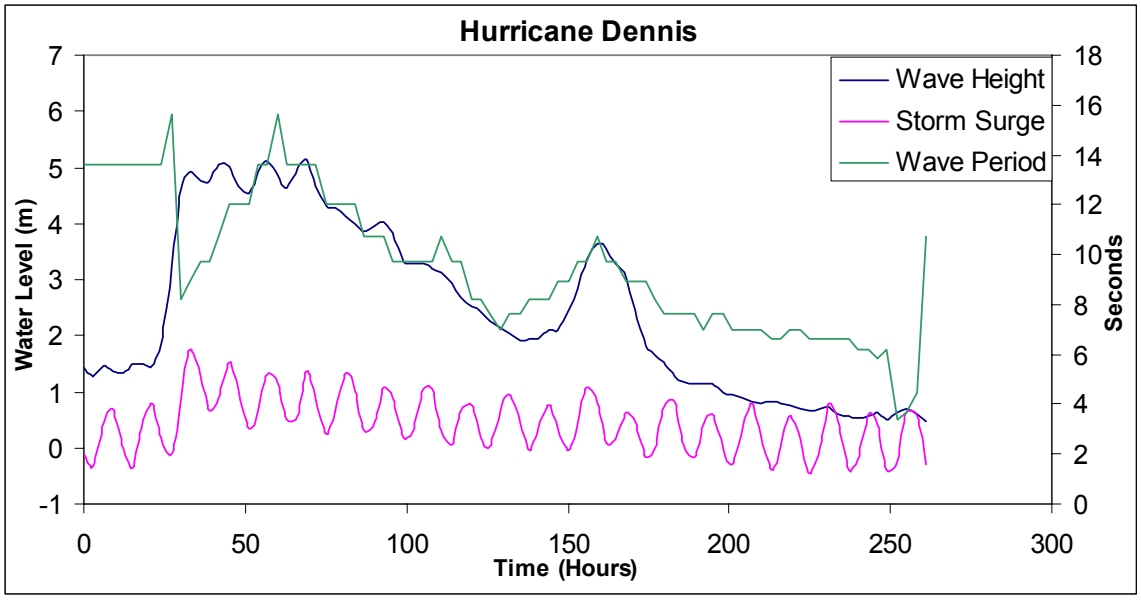

Figure 7.1. Hurricane Dennis data.

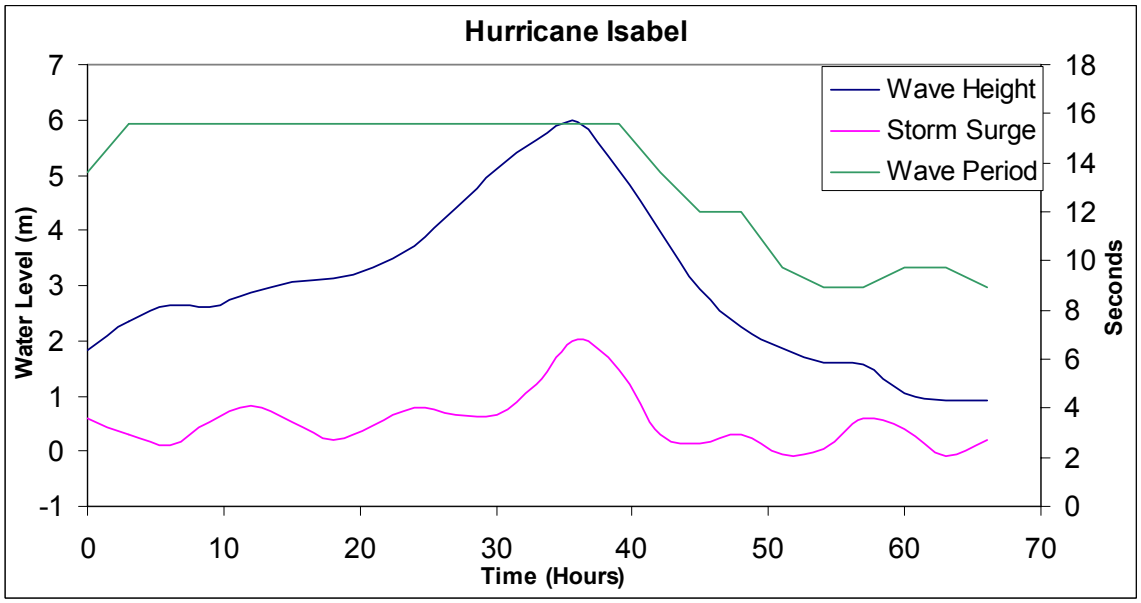

Figure 7.2. Hurricane Isabel data.

7.4 Wave Angle

Wave angle is an input parameter that both models consider and require the user to define. At the Buxton site no directional data was available, and at the FRF site since the angle of incidence is measured from directional wave gauges in deep water, no knowledge about wave orientation at the shoreline was known. For these reasons all waves were modeled to be normally incident at both sites. This may cause both models to over predict the erosion caused by the storm events.

8. METHODOLOGY

The evaluation of the SBEACH and COSMOS models required the acquisition of profile data as well as wave and water level data, calibration to each of the two study sites, and model simulations. Results from both models were compared to the measured post-storm profiles, which were assumed to represent the change that resulted from the storm event. The evaluation of each model was based on visual inspection and quantitative analysis. Quantitative analysis included a comparison of the predicted and measured percent volume change within specified boundaries on the subaerial portion of each profile. A comparison between the predicted and measured waterline recession was also made for each profile.

After the input data (profile, wave and water level) was obtained, a calibration procedure was preformed on both models using a single transect from each location. The procedure included a model run using default calibration values. The model results were compared to the final measured profile. Then values were adjusted for each calibration parameter in an attempt to improve results. The SBEACH CALIBRATION and COSMOS CALIBRATION chapters describe the calibration at the Buxton site using transect AA.

Once each model was calibrated, model simulations were performed. Results produced by both SBEACH and COSMOS were compared to the measured post-storm profiles. The cases presented in the Results chapter are those which display the most significant changes between pre and post-storm measurements in the subaerial portion of the profile, which includes the dune and beach face. In cases where

significant erosion of the dune occurred as a result of the storm, additional analysis focused on the dune.

For each case presented, four profiles were entered into a program developed for the purpose of analyzing beach morphology called BMAP. BMAP is discussed in section 8.3. The profiles were labeled Initial (pre-storm profile), Final (post-storm profile), SBEACH (predicted post-storm profile computed by SBEACH), and COSMOS (predicted post-storm profile computed by COSMOS). BMAP calculated profile volumes between defined boundaries. The percent difference between the pre and post-storm volumes are referred to as the actual percent volume change. The percent volume change between the initial profile and the SBEACH and COSMOS predicted profiles were compared to the measured actual percent volume change. BMAP also provided the location of the waterline on each profile. The difference between the waterline location on the post-storm profile and the initial profile is the waterline recession.

Figure 8.1 depicts how boundaries were defined to calculate profile volumes using BMAP. Boundaries such as those within the blue box were defined to quantitatively analyze selected cases. The region within the blue box includes the dune as well as the beach face and is bounded by the waterline, and the point on the backside of the dune referred to as the landside point. The landside point is either the location of the dune heel or the Data Intersection point depending on the source of the profile data. The Data Intersection point is discussed later in this chapter.

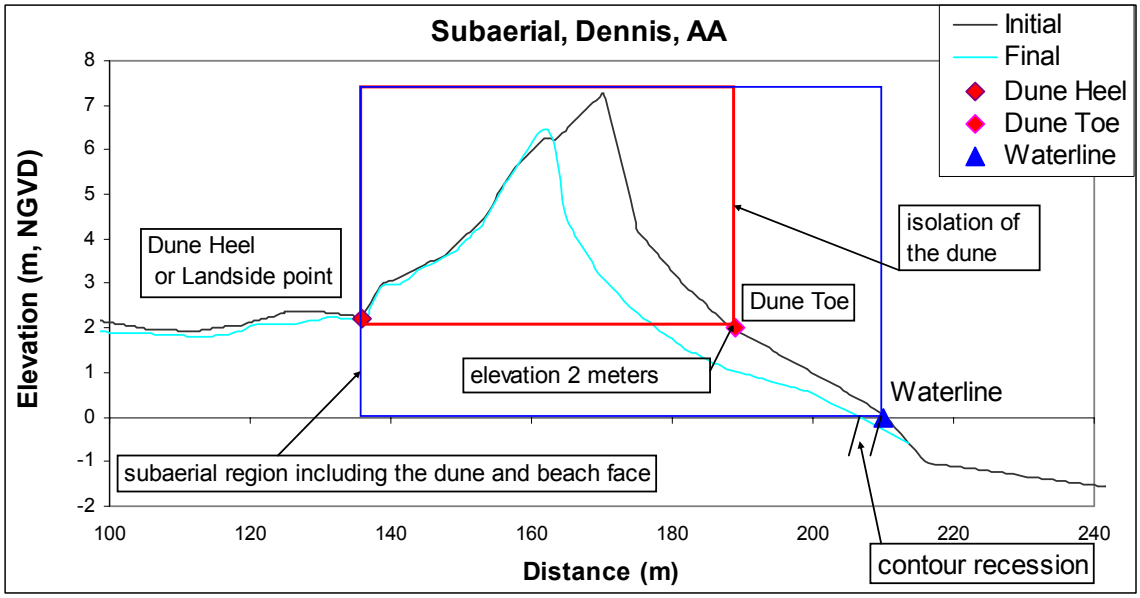

Figure 8.1. Example subaerial profile view.

Additional analysis using BMAP was performed to isolate the dune feature where significant erosion occurred. To isolate the dune on a particular profile, the toe and heel of the dune were identified on the pre-storm profile. The dune toe is the point where the dune begins on its seaward face, and the heel is where it ends on the backside of the dune. Identification of the toe and the heel is a subjective process. Generally, inflection points, such as where the slope of the beach profile sharply increases upward, identify the dune toe. However, it is easy to mistake the initial point of a substantial berm for the dune toe. In Figure 8.1, the toe and heel of the dune on profile AA are indicated with red diamonds. When using BMAP to calculate dune volume, the elevation of the dune toe was used as the lower vertical boundary for the red box in Figure 8.1. Otherwise the lower vertical boundary was the elevation of the pre-storm (Initial profile) waterline.

Transects from the FRF location were created by merging two datasets. The procedure is explained in section 9.3.2. The intersection points of the two datasets

were used as the landside point instead of the heel of the dune to analyze transects. These intersection points are marked in all figures containing FRF profiles and are labeled “Data Intersection”.

8.1 Rating System and Consideration of Uncertainties

For each case, the predictions from SBEACH and COSMOS were assigned a rating based on how closely each predicted the actual measured percent volume change within the boundaries specified. A rating of “good” was assigned if the model predicted the actual measured volume change within 15 %. A rating of “fair” was assigned if the predicted value was within 25 % of the actual measured value, and if the predicted value deviated more than 25 % from the measured volume change a rating of “poor” was assigned. These limits were determined by considering the variation in model results produced by a range of uncertainty associated with both wave angle and mean sediment grain size. The uncertainties associated with both of these factors are discussed in sections 8.1.1 and 8.1.2.

Model performance in the prediction of waterline recession was generalized and described as either a “reasonable” or an “unreasonable” prediction. Generalized descriptions were used because of uncertainty associated with both wave angle and mean grain size as well as the variation in waterline location due to tidal fluctuation. If a model’s prediction was within 20 m of the measured post-storm waterline a rating of “reasonable” was assigned. A rating of “unreasonable” was assigned if a model predicted the post-storm waterline to be greater than 20 m from where it was measured.

8.1.1 Uncertainty Associated with Wave Angle

As mentioned in section 7.4, all waves were considered to be normally incident to the shore. However, this is a simplification due to the lack of accurate data. During an actual storm event, waves approach the shore at varying angles of incidence. An effort was made to consider the effect of introducing a mean wave angle on model results.

A maximum likely mean wave angle was first determined. Using the average wave direction (relative to true north) recorded by gauge 3111 during each storm and the geographical orientation (relative to true north) of the FRF site, an estimate of the maximum likely mean wave angle was made. From wave records for Hurricane Dennis and Hurricane Isabel, the mean wave directions were 86 and 89 degrees respectively. Those values, relative to shore normal, are 4 degrees and 1 degree respectively. The geographical orientation of the FRF site is about 18 degrees west of true north (FRF website, 2003). After the site orientation adjustment, the mean wave angles became 14 and 17 degrees for Hurricane Dennis and Hurricane Isabel respectively. The larger wave angle, 17 degrees, was rounded up to 20 degrees and was used to identify a range of variation in model results associated with wave angle.

A comparison between results using normally incident waves and waves with a 20 degree angle of incidence was made at both sites. The results are presented in Table 8.1 and were used in the development of the rating criteria discussed in section 8.2. The wave angle has negligible effects on SBEACH results in terms of both percent volume change and waterline recession. However, the use of a wave angle in the COSMOS model caused a 25 % change in results at the FRF and a 16 % change

at Buxton. Waterline recession predicted by the COSMOS model is also more sensitive to wave angle than in the SBEACH model, 9 m and 6 m verses 1 m and 0 m.

Table 8.1. Relative effect of a 20 degree wave angle.

Location	Percent Volume Change		Waterline Recession (m)	
	SBEACH	COSMOS	SBEACH	COSMOS
FRF	1	25	1	9
Buxton	1	16	0	6

8.1.2 Uncertainty Associated with Mean Sediment Size

The variation in sediment size at the FRF is discussed in section 9.2 and again in Appendix B. It was difficult to assign a single grain size to the FRF study site based on the information presented in those two sections. Therefore, the effect of grain size on model results was evaluated by a test of a limited range of values around the actual value used. However, since increasing the grain size above 0.80 mm at the FRF did not change the SBEACH result, the range of values tested was 0.60 mm to 0.80 mm.

Table 8.2. Variation in model results due to adjustment of grain size. (Actual grain sizes used are in bold print.)

Grain Size (mm)	Percent Volume Change		Waterline Recession (m)	
	Results using Buxton Transect AA			
	SBEACH	COSMOS	SBEACH	COSMOS
0.35	31	51	-1	-36
0.45	22	41	2	-32
0.55	13	36	3	-27
Range	**18**	**15**	**4**	**9**
Results using FRF line 58				
0.60	18	48	-1	-26
0.70	5	44	0	-24
0.80	0	40	0	-23
Range	**18**	**8**	**1**	**3**

Table 8.2 presents results from both SBEACH and COSMOS for the range of grain sizes tested. Results from Buxton transect AA and FRF line 58 are presented.

The range of percent volume change values produced by SBEACH was 18% at both study sites. The COSMOS model predicted a 15 % range at Buxton and an 8 % range at the FRF. The range of predicted contour recession values by SBEACH was 4 meters and 1 m for Buxton and the FRF respectively. The range of waterline recession values predicted by COSMOS was 9 m and 3 m respectively. As far as volume change, SBEACH displayed more sensitivity to grain size. In terms of waterline recession, SBEACH did not show as much variation as COSMOS.

8.2 Rating Criteria

Once the extent of result variation associated with both wave angle and grain size selection was identified, a criterion for the rating system used in the Results chapter was defined. The largest change in models results from either wave angle or uncertainties associated with grain size was 25 %. This value came from using a wave angle of 20 degrees instead of 0 degrees in the COSMOS model at the FRF. Based on that, a value of 25 % was used as the maximum percent difference between the predicted and measured post-storm profiles for a "fair" performance rating. If the predicted value deviated more than 25 % from the measured value, the model performance was rated as "poor". To receive a performance rating of "good" the predicted percent change had to be within 15 % of the measured percent change. That value was selected because it was reasonably within the range of variation associated with both grain size and wave angle in almost all the cases in Tables 8.1 and 8.2.

The maximum change in contour recession resulting from either wave angle or uncertainties associated with grains size was 9 m. The horizontal error associated

with waterline fluctuations due to the tidal cycle was estimated to be about 11 m (see Appendix D for description of horizontal error). The sum of these two variables, 20 m, was used as the maximum differential between the predicted value and the measured value for a rating of "reasonable". If the predicted waterline location was in excess of 20 m from the measured location, the model received a performance rating of "unreasonable".

8.3 The Beach Morphology Analysis Package (BMAP)

In most of the cases presented in the Results chapter the Beach Morphology Analysis Package or BMAP was used to calculate subaerial volumes and track contour changes between pre and post-storm profiles. The BMAP program was developed by the US Army Corps of Engineers and is available through Veri Tech, Inc.

The program has many tools used to analyze dynamic and morphologic changes associated with beach profiles (Veri Tech website, 2004). Used here was a tool which calculates volumes within specified boundaries. The resulting volumes were used to calculate percent volume change relative to the initial profile. Included in the BMAP results is the location along the x-axis of the elevation contour of the waterline, specified by the user, for each profile. These values were used to determine waterline contour change.

9. SEDIMENT AND PROFILE DATA

9.1 Buxton

Sediment data was provided by NCDOT (Overton and Fisher, 2000). Field samples were collected at the north, middle, and south end of the Buxton site. They were taken from the top few centimeters of the surface at several points across the subaerial portion of the beach; the top of the dune, toe of the dune, the beach face, and the water's edge. Sieve analysis was performed at the NCDOT Soils Laboratory. Grain size distributions from each sample were plotted on semi-log graph paper and from these plots the author selected mean grain sizes. These mean values are displayed in Table 9.1.

Table 9.1. Mean grain sizes at Buxton, Phi units.

	Dune Top	Dune Toe	Beach Face	Water Edge	Average Value for Buxton Area
Buxton					
North	1.1	0.85	x	1.6	
Middle	1.1	0.8	1.3	1.5	
South	1.1	0.9	1.6	1	
					1.17 (0.45 mm)

For both SBEACH and COSMOS, a mean grain size of 0.45 mm was used for all Buxton simulations.

9.2 Duck

The sediment sizes found at the FRF site vary widely in the cross-shore direction. Medium sized sand and small pebbles are primary found on the beach and in shallow water close to the shore, and in nearshore the sediment tends to be composed of fine and very fine sand (FRF website, 2004).

On the FRF website some sediment data is available for download. The dataset selected here consisted of sediment data that was collected between March

1984 and September 1985 along two profile lines (FRF lines 62 and 188). Though this dataset was not the most recent data available, it was selected because it included samples from the dune out to 8 m of water depth, and the collection period covered more than a full year. The most recent sediment data available online at the FRF website was collected during the SandyDuck Sediment Experiment in 1997. Data collection during this experiment consisted of mainly subaqueous samples.

During the 1984-1985 collection period, samples were collected twenty-one times along each line. During each survey approximately seventeen grab samples across both profiles were collected. Mean grain sizes in both millimeter and phi units are provided in the data files which are downloadable. The data shows significant variation in mean sediment size both in cross-shore direction and in time.

Over the eighteen months that samples were collected, mean sediment diameters were very inconsistent, Figure 9.1. In order to determine a representative subaerial grain size to use in the models the author made two decisions on how to use this sediment data. First it was decided to only include samples that were collected either on the subaerial beach or in less than 3 m of water depth. This was done to place more emphasis on the characteristics of the portion of the profile that is of interest here. Second, mean values collected throughout the 1984 to1985 period would be used to determine the mean sediment diameter. This was done so that the grain size would be representative of the variation in time since the collection period was not around the same time as either storm event.

Figure 9.1 is a plot of mean grain sizes from grab samples collected between the dune and three meters of water depth along line 62 between March 1984 and September 1985.

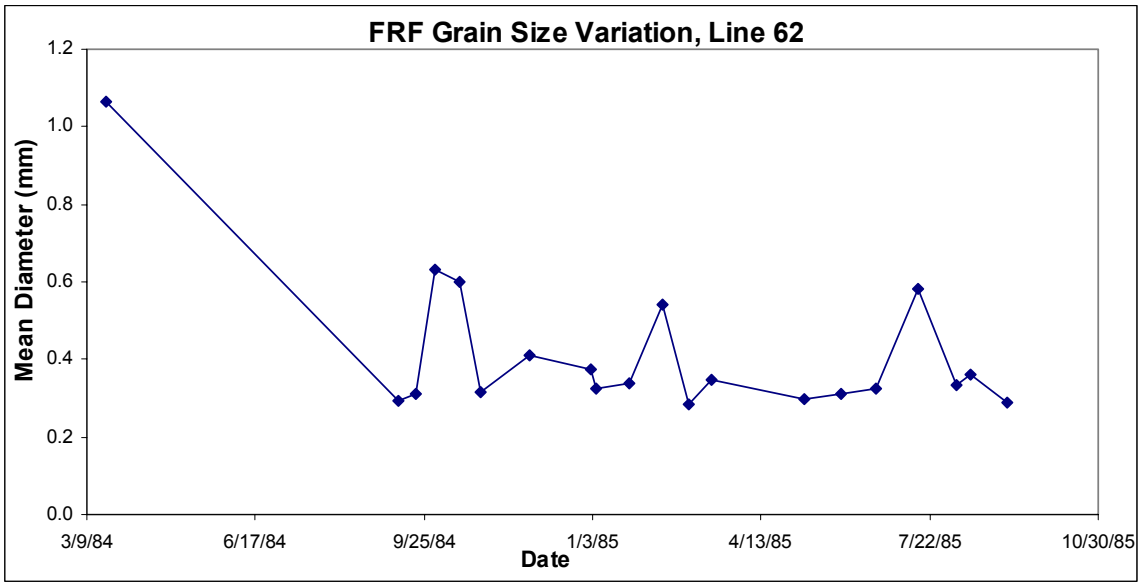

Figure 9.1. Variation of mean grain size between March 1984 and September 1985, including samples only to 3 m of water depth.

Representative grain sizes were determined by taking the average of all the mean values provided within the data files for subaerial samples as well as samples collected in less than 3 m of water. The values obtained for FRF lines 62 and 188 were 0.42 mm and 0.46 mm respectively. Transects on the north end of the property (58 and 62) were modeled using a representative grain size of 0.42 mm and transects on the southern end of the property (166, 174, 176, 188, and 190) were modeled using a representative grain size of 0.46 mm.

With these grain size values, both models produced mostly good or fair results for simulations of Hurricane Isabel at the FRF site, however both produced poor results for simulations of Hurricane Dennis. Attempts to improve model performance

through calibration were unsuccessful. Adjustment of the estimated mean grain size did, however, improved model performance. Sensitivity to the grain size parameter for both models was investigated and results are provided in Appendix B. Based on results from that investigation the representative grain size value was increased to 0.80 mm for simulations of Hurricane Dennis at the FRF. Though this adjustment to grain size was relatively large, the value used was within the range of grain sizes found at that location. Table 9.2 lists the mean grain size values used at each transect for each storm event.

Table 9.2. Mean grain sizes for FRF transects, units in (mm).

Profile ID	Dennis	Isabel
58	0.80	0.42
62	0.80	0.42
166	N/A	0.46
174	N/A	0.46
176	N/A	0.46
188	0.80	0.46
190	0.80	0.46

9.3 Profile Data

Profile data for this research came from several different sources. At each of the two study locations both pre and post-storm profile data was obtained. The pre-storm data was used as part of the input to each of the models, the post-storm profile data was considered to be a measurement of the change resulting from the storm event.

9.3.1 Buxton

This section describes the dataset used to analyze the impacts of Hurricane Dennis on the Buxton area. This data was provided from both NCDOT and the Wilmington District of the U.S. Army Corps of Engineers to Dr. Margery Overton

and Dr. John Fisher to be used in a highway vulnerability study which they completed in August 2000 (Overton and Fisher, 2000).

The subaerial profile data for the Buxton site was created using digital photogrammetry. With this technology, digital terrain models (DTM) can be created using aerial photographs (Overton and Fisher, 2003). These aerial photos are routinely taken along the Outer Banks of North Carolina for the purpose of monitoring the long-term movement of the coastline. A series of aerial photos were taken in 1998 by NCDOT, and from those NCDOT created the DTM which was used as the pre-storm subaerial dataset. It should be pointed out that Hurricane Dennis did not strike the Outer Banks until a year after the photos were taken, during which changes in the initial profiles may have occurred that did not result from the storm event itself. After Hurricane Dennis hit the Outer Banks, another digital photogrammetric mission was flown over the Buxton area by NCDOT so that the effects of the storm could be analyzed. The DTM from these photos were used as the post-storm subaerial dataset. Subaqueous data was obtained from bathymetric surveys that were conducted during the spring of 2000 by the Wilmington District of the U.S. Army Corps of Engineers (Overton and Fisher, 2000). Actual pre-storm bathymetry was not available for this site.

For analysis at Buxton, several pre and post-storm subaerial profiles were derived from the DTM by Overton and Fisher (2000). In this study, three of those transects were used to test the performance of both cross-shore numerical models. The transects are labeled AA, CC, and LL. Transect AA is the northern most transect, CC is about 300 m to the south of AA, and LL is about 1700 m south of CC

(Overton and Fisher, 2000). A possible source of error associated with the Buxton dataset is that both transects CC and LL may have been altered by NCDOT road maintenance crews before the post-storm aerial photos were taken. After Hurricane Dennis struck, sediment was washed onto NC 12 in many areas including Buxton. As a result, the next day clean up crews used bulldozers to move the sediment off the road and back onto the beaches. It can not be said for certain that either CC or LL was in fact altered by this activity but it is possible. According to Overton and Fisher (2000), at transect AA there were no post-storm repairs made to the dune or beach.

9.3.2 Duck

At the FRF in Duck, North Carolina, 26 shore-normal profile lines are surveyed monthly. Seven of the those lines were selected to be used here, lines 58 and 62 are located approximately 585 and 485 m, respectively, north of the landward end of the pier. The pier at the FRF is a 560 meter long, shore normal concrete structure in the middle of the property. Lines 166, 174, 176, 188, and 190 are located approximately 5, 105, 455, 515, and 605 m, respectively, south of the landward end of the pier. Table 9.3 lists the dates that surveys were taken around each storm at the FRF location.

Table 9.3. FRF survey dates.

	Dennis		Isabel	
Profile ID	Pre-Storm	Post-Storm	Pre-Storm	Post-Storm
58	7/19/1999	9/24/1999	8/8/2003	9/21/2003
62	7/19/1999	9/24/1999	8/8/2003	9/21/2003
166	7/21/1999	9/25/1999	8/8/2003	9/22/2003
174	7/19/1999	9/25/1999	8/8/2003	9/21/2003
176	7/19/1999	9/25/1999	8/8/2003	9/21/2003
188	7/20/1999	9/24/1999	8/8/2003	9/21/2003
190	7/20/1999	9/24/1999	8/8/2003	9/21/2003

Surveys conducted at the FRF extend from the dune out to deepwater. Because the dunes are rarely affected by waves, in most cases the FRF surveys do not extend past the top of the dune. To ensure that the landward extent of the profiles were beyond the maximum possible up-rush limit of any wave condition during either storm each profile was extended landward 152 meters using data from a 1998 DTM provided by the North Carolina Division of Coastal Management (DCM) (Overton and Fisher, 2004). The landward most point from each FRF profile survey was used as a starting point to continue the profile further landward using the DTM data. The point of intersection between the FRF data the DTM data is marked on all FRF profile figures with a vertical line labeled "Data Intersection". When using the BMAP program to analyze the FRF profiles, the Data Intersection points for the pre-storm profiles were used as the landward boundary, instead of using the heel of the dune as was done at Buxton.

10. SBEACH CALIBRATION

Table 10.1 lists calibration parameters that are adjustable in the SBEACH model for the purpose of improving model performance specific to a location. SBEACH calibration parameters include; the sediment transport rate coefficient, coefficient of slope dependent term, and the depth of foreshore. The remaining variables listed in the table are adjustable in the model but are not labeled as calibration parameters. The spatial rate of decay affects the decay of wave height within the surf zone, the avalanching angle effectively places a limit on the maximum allowable slope on a profile. Mean grain diameter is a value intended to represent the mean size of the sediment found at the study site. Table 10.1 includes a default value, a range of values allowable, and the value which was used at each location.

Table 10.1. SBEACH Input Parameters

Parameter	Symbol (units)	Default Value	Value at Buxton	Value at FRF	Range
Transport rate coefficient	K (m^4/N)	1.75x10^-6	1.75x10^-6	1.75x10^-6	2.5x10^-7 to 2.5x10^-6
Coefficient of slope dependent term	€ (m^2/sec)	0.002	0.005	0.005	0.001 to 0.005
Landward depth of foreshore	DFS (m)	0.3	0.3	0.3	0.15 to 0.5
Spatial rate of decay	λ	0.5	0.5	0.5	0.1 to 0.5
Max avalanching angle	(degrees)	45	25	45	15 to 90
Mean grain diameter	D50 (mm)	0.35	0.45	(Varies)	0.15 to 1.00

The sediment transport rate coefficient has units of volume of sediment per unit force per unit length of beach, ($\frac{m^4}{N}$). Increasing this value causes the profile evolution to approach its equilibrium shape more rapidly. As discussed in Larson and

Kraus (1989), a higher transport rate significantly increases both the bar height and bar volume in the earlier time steps, though does not necessarily impact the final equilibrium bar volume or height depending on storm duration. The slope-related sand transport term, ϵ, is related to the slope of the profile, it has units of square meters per second. A large value of ϵ infers a flatter equilibrium beach profile meaning more sediment is to be moved offshore (Larson and Kraus,1989).

Depth of Foreshore, DFS, is the depth at the location where the region of broken waves ends and the swash zone begins. Increasing this value translates to a larger swash zone which will normally increase erosion on the foreshore (Larson and Kraus, 1989).

10.1 Calibration to Buxton

The calibration process involves selecting one profile from a study site and varying the calibration parameters in an attempt to improve the performance of the model at the given site. Figures 10.1 through 10.5 graphically show the effects when the above variables are adjusted. All figures are zoomed into the subaerial portion of the profile as that is the focus of this work. Effects of the following variables were judged based on visual inspection of the subaerial portion of the profile. Initially default values were used for each parameter, and then that value was varied to see if the model result more closely resembled the measured post-storm profile. If improvement could be clearly seen the adjusted value was used, otherwise the default value was used. Transect AA from Buxton was selected for the calibration process.

At the Buxton location Figures 10.1 and 10.4 indicate that changing the default value for both the sediment transport rate coefficient and the spatial rate of

decay coefficient did not improve the match between the predicted result and the measured result. Figure 10.2 indicates that the SBEACH prediction of the beach face is improved when using a value of 0.005 for the slope dependent term. Figure 10.3 shows that the prediction of the dune height is closer to that which was measured when a value of 0.5 m was used for the depth of the foreshore. Figure 10.5 displays the influence that the avalanching angle has on the subaerial region. At the Buxton site an angle of 25 degrees resulted in the best match with the final post-storm dune profile.

Through the calibration process the values for the three calibration parameters as well as the spatial rate of decay and avalanching angle were determined. Calibration was preformed at both study sites and the values used at each location for each parameter are listed in Table 10.1.

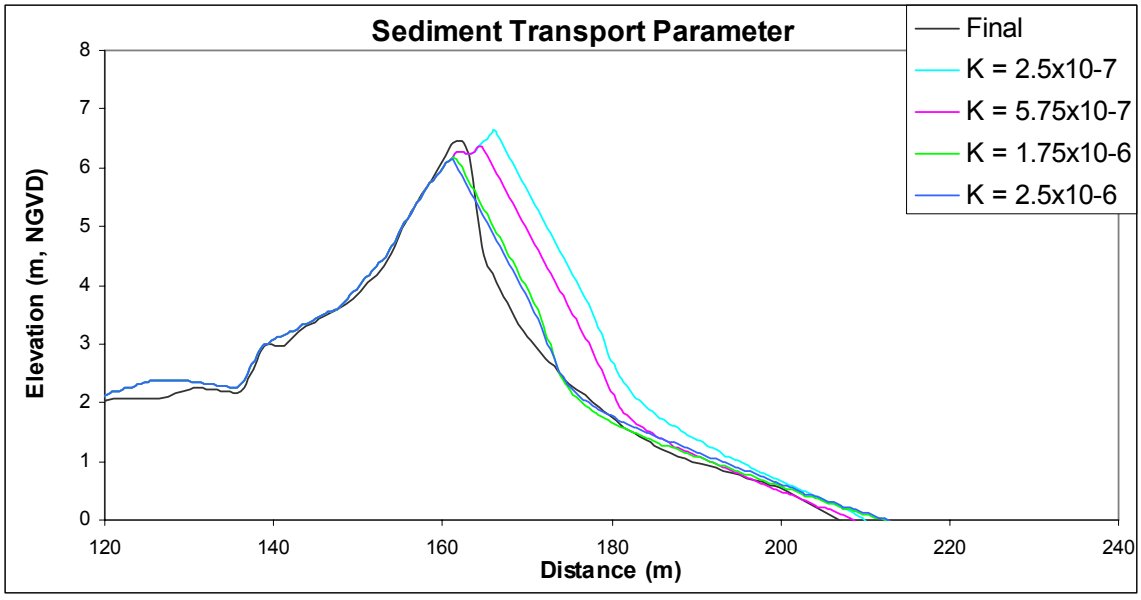

Figure 10.1. Effects of varying the sediment transport rate coefficient, K.

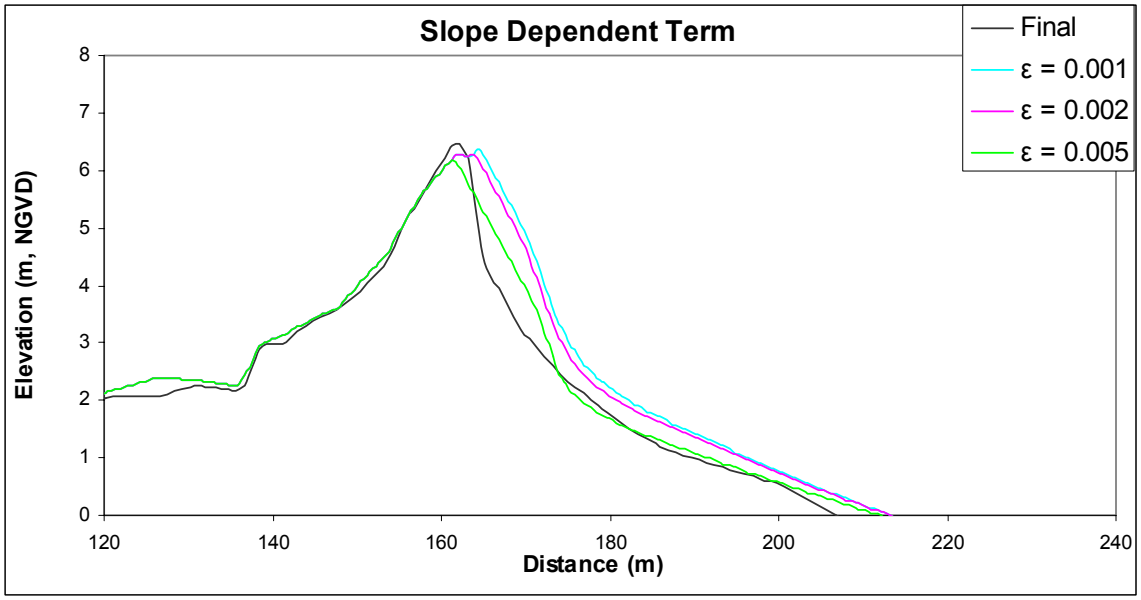

Figure 10.2. Effects of varying the coefficient of the slope dependent term, ε.

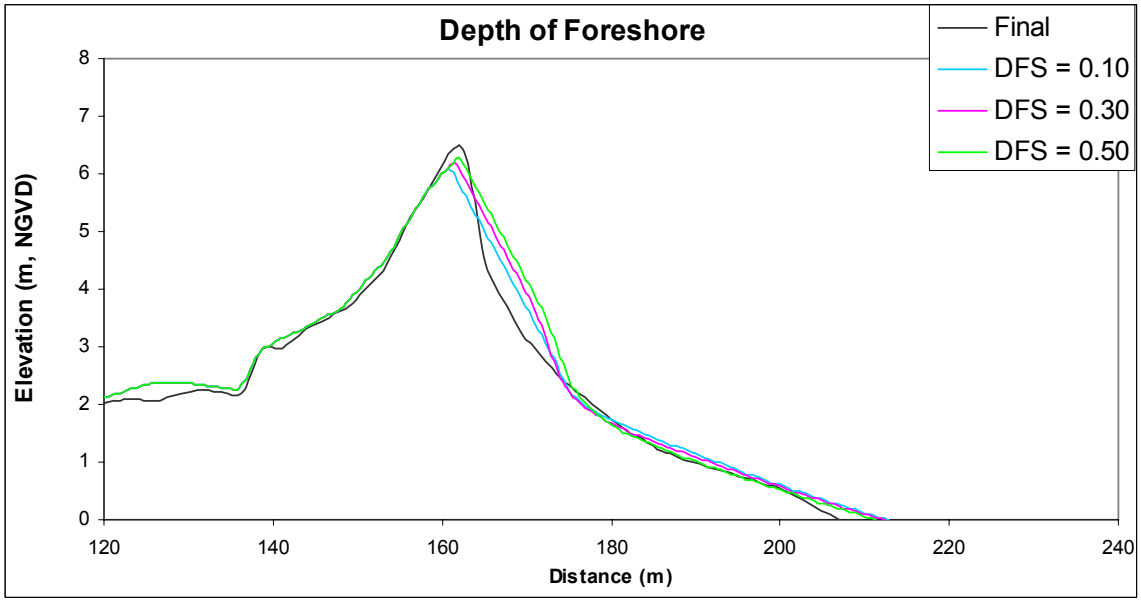

Figure 10.3. Effects of varying DFS.

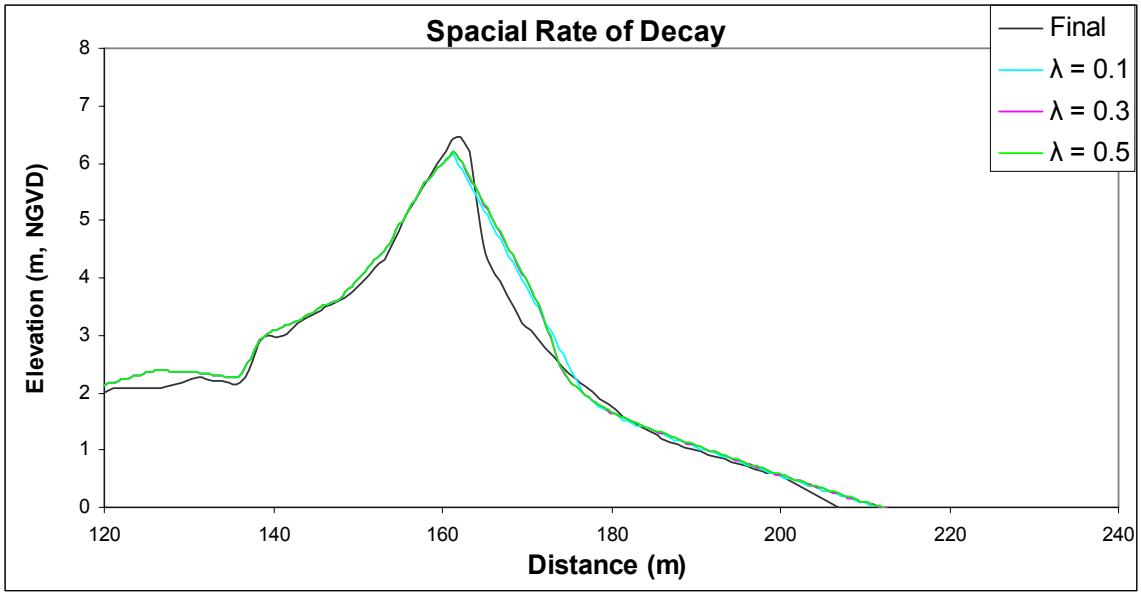

Figure 10.4. Effects of varying the spatial rate of decay coefficient, λ.

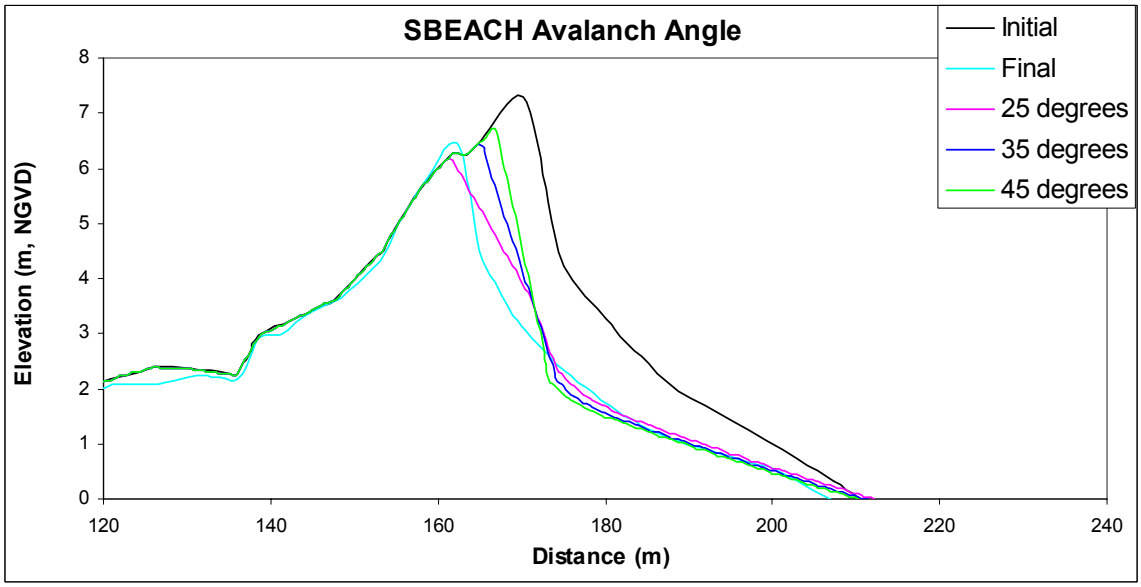

Figure 10.5. Effects of varying maximum avalanching angle.

11. COSMOS CALIBRATION

In the COSMOS model there are two variables that are considered calibration parameters, the suspended and bed load efficiency factors. These variables along with other adjustable parameters, that are intended to represent characteristics of the study site, are listed in Table 11.1. The remaining parameters are; sediment angle of repose, the depth beyond which no sediment transport calculations are preformed, the maximum avalanching angle, and the residual avalanching angle. Sediment porosity is also available for the user to define.

Table 11.1. COSMOS Parameters.

Parameter	Default Value	Value at Buxton	Value at FRF	Range
1 - Porosity	0.6	0.7	0.7	0.65 - 0.75
Angle of Repose	0.63	0.78	0.63	0.50 - 0.78
Bed load efficiency	0.1	0.1	0.1	0.06 - 0.14
Suspended load efficiency	0.02	0.02	0.02	0.016 - 0.022
Avalanching Angle	26	35	35	35 - 20
Residual Angle	18	18	25	18 - 22
Depth of Calculations	0.26	0.46	0.26	0.10 - 0.76

11.1 Calibration to Buxton

The figures presented in this section were used to determine the most appropriate values for the listed parameters (Table 11.1) at the Buxton location. Again transect AA was used for the calibration process. All figures are zoomed into the subaerial portion of the profile. Effects of the following variables were judged based on visual inspection of the subaerial profile. Initially default values were used for each parameter, and then that value was varied to see if the model result more

closely resembled the measured post-storm profile. If improvement could be clearly seen the adjusted value was used, otherwise the default value was used.

Figure 11.1 indicates that increasing suspended load efficiency factor resulted in greater dune and foreshore erosion. Decreasing this value did appear to reduce the predicted erosion of the beach face, however, it did not improve COSMOS's estimate of the post-storm dune. In this case the author decided to use the default value.

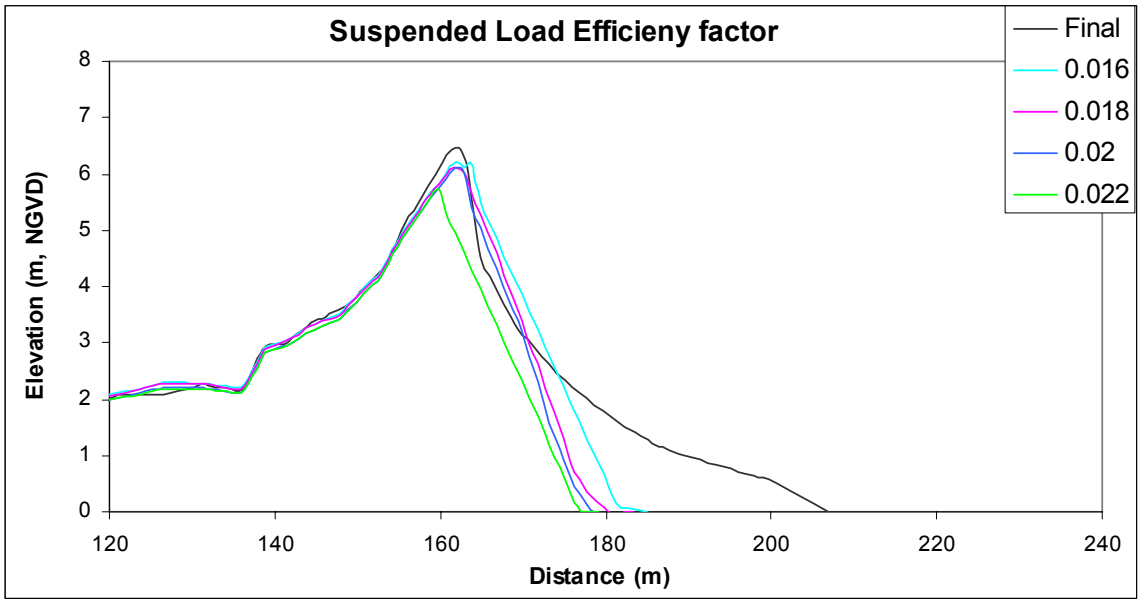

Figure 11.1. Effect of varying the suspended load efficiency factor.

Figure 11.2 shows that changing the value of the bed load efficiency factor had very little effect on the results. For the bed load efficiency factor the default value was also used.

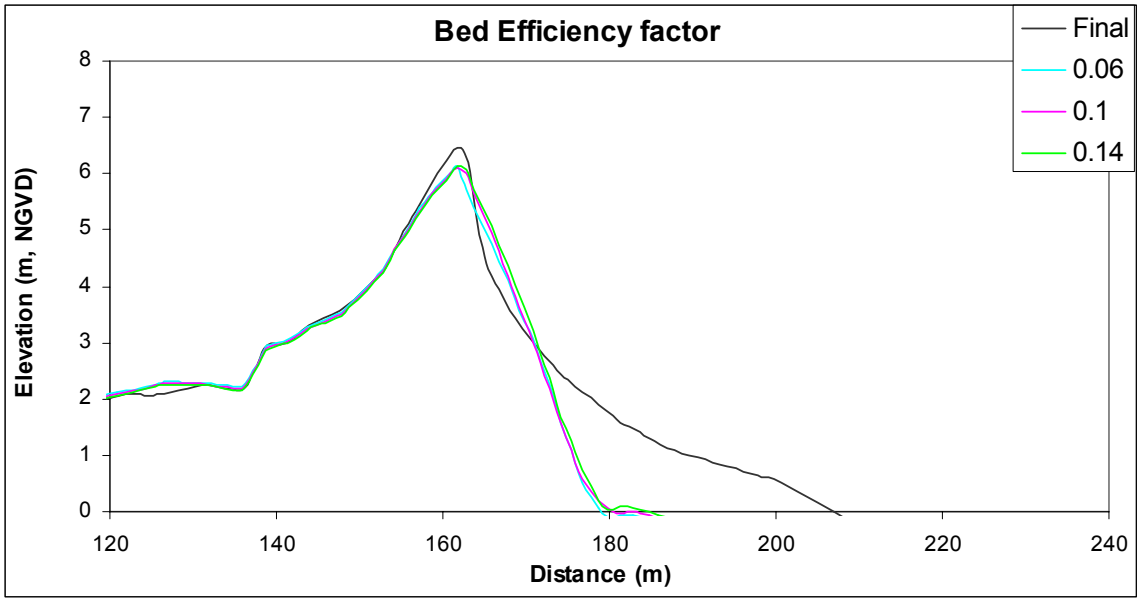

Figure 11.2. Effect of varying the bed load efficiency factor.

When the sediment slope of repose, the maximum angle that the sediment will achieve before slumping, variable was increased, the prediction on the upper portion of the dune improved slightly while the predicted waterline recession was about the same as with the default value. For this case the value used in the model was increased to 0.78, or 38 degrees.

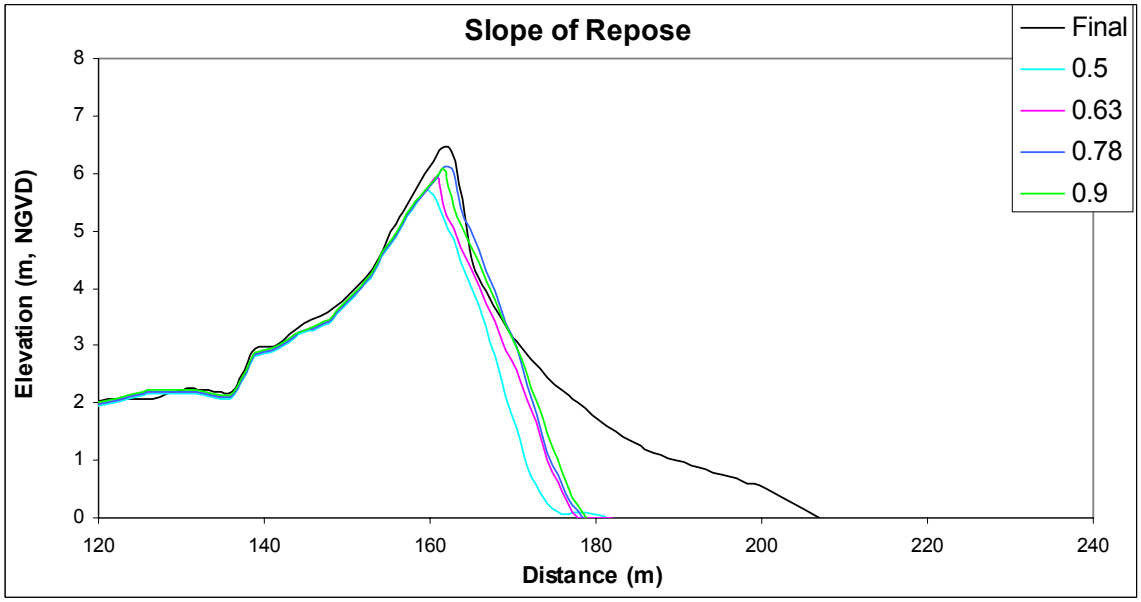

Figure 11.3. Effect of varying the slope of repose.

At the landward end of a profile, a depth is defined, beyond which no further sediment transport calculation will be made. Landward of that point the sediment transport rate is extrapolated to zero at the up-rush limit for each wave condition (Southgate and Nairn, 1993). Figure 11.4 indicates that increasing this depth from its default value (0.26 m) resulted in less recession of the waterline and less dune erosion. The author decided that the 0.46 m value produced the best match with the measured post-storm profile.

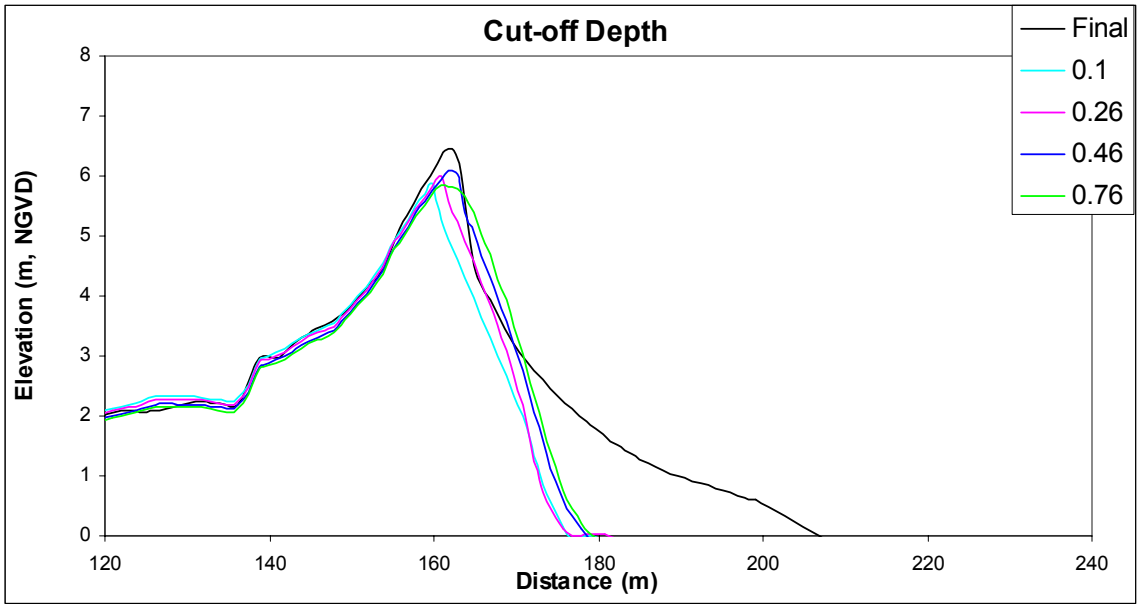

Figure 11.4. Effect of varying the cut-off depth.

Figure 11.5 shows the influence of the avalanching angle on model results. Each profile on the figure is label with the maximum avalanching angle and followed by a slash and then the residual angle. At the Buxton location an avalanching angle of 35 degrees with a residual angle of 18 degrees (purple line) appeared to fit best when taking both the dune area as well as the waterline recession into account.

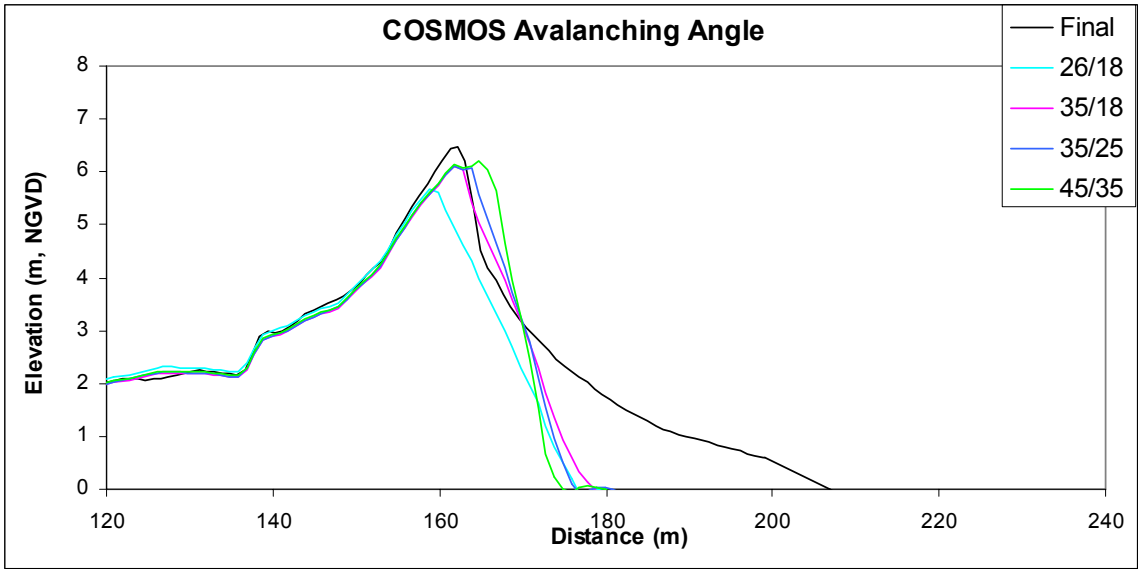

Figure 11.5. Effect of varying the Avalanching angle.

Through the calibration process the values of the two calibration parameters as well as the sediment slope of repose, the cut off depth for transport calculations, and avalanching angle were determine. Calibration was preformed at both study sites and the values used at each location for each parameter are listed in Table 11.1.

12. RESULTS

The primary focus of this study was to evaluate each of the model's ability to replicate the measured post-storm subaerial beach profile and estimate the volume of material removed. Subaerial changes were evaluated both visually and quantitatively. Visual comparison was done simply by plotting model outputs and comparing those results to the measured post-storm profile. Quantitative analysis was preformed by comparing how accurately each model predicted the volume of material removed and the recession of the waterline (positive values in the waterline recession column indicate accretion and negative values indicate erosion). Data that was collected from two North Carolina study sites and wave and water level information for both Hurricane Dennis and Hurricane Isabel recorded at the FRF was used in this research.

12.1 Buxton

12.1.1 Transect AA

Transect AA is the northern most profile in the study area and was also the one with the largest pre-storm dune. The actual measured subaerial volume change between the pre and post-storm profiles landward of the waterline and in front of the dune heel was 26 %. SBEACH's prediction was within 4 % of that value, and COSMOS's prediction was within 15 % of that value. In accordance with the criteria defined in the Methodology chapter of this report, the performance by both SBEACH and COSMOS was rated as good. The SBEACH model predicted the waterline to be 5 m seaward if where it was actually measured to be. This value was within the reasonable range defined in the Methodology chapter. The COSMOS model

predicted a 32 m recession of the waterline while only a 3 m recession was measured, a difference of 29 m, which according to the criteria, was an unreasonable prediction.

Table 12.1. Subaerial results, Buxton Profile AA, Hurricane Dennis

Profile Name	Heel (m)	Waterline (m)	Volume (cu. m/m)	Percent Volume Change	Waterline Location (m)	Waterline Recession (m)
Initial (AA)	136	210	253	0	210	0
Final (AA)	136	210	188	26	207	-3
SBEACH (AA)	136	210	197	22	212	2
COSMOS (AA)	136	210	150	41	179	-32

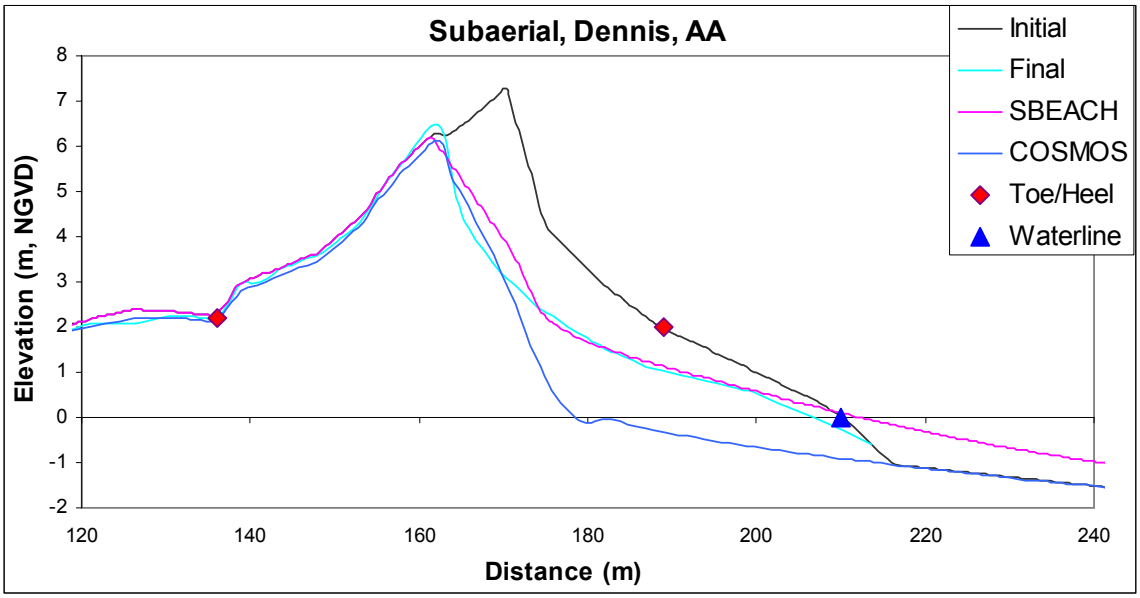

Figure 12.1. Effects of Hurricane Dennis on transect AA.

Further analysis was performed on this profile because from Figure 12.1, visible dune erosion occurred. The toe and heel are marked in Figure 12.1, the base of the dune was over 50 m wide and the crest was in excess of 7 m above the waterline. Table 12.2 shows the initial, final, and predicted dune volumes measured between the toe (at 189 m) and the heel (at 136 m) above the 2 m contour (elevation of the dune toe). The table also lists the percent volume change but does not list the contour recession since the contour in this case was the dune toe and not the

waterline. The measured percent volume change after the storm was 38 %. Both models predicted a percent change that was within the range of good.

Table 12.2. Dune results, Buxton AA, Hurricane Dennis

Profile Name	Heel(m)	Toe(m)	Volume (cu. m/m)	Percent Volume Change
Initial (AA)	136	189	126	0
Final (AA)	136	189	78	38
SBEACH (AA)	136	189	85	32
COSMOS (AA)	136	189	73	42

12.1.2 Transect CC

Transect CC was located approximately 300 m south of AA (Overton and Fisher, 2000). Figure 12.2 displays the measured results as well as the results predicted by each model. Unlike at transect AA, the two models show virtually no agreement in the subaerial portion of the profile. SBEACH predicted the dune to be completely removed from its original location while making a reasonable estimate of the post-storm waterline position, 1 m of recession. The COSMOS result indicated that some of the dune would remain but predicted a 26 m recession of the waterline, which was considered to be unreasonable. The actual measured waterline location was about one half a meter seaward of its pre-storm position. Neither model was in agreement with the measured post-storm subaerial profile. However, this may be because this transect could have been altered by maintenance crews before the post-storm data was recorded. Because of this uncertainty quantitative analysis was not preformed for transect CC.

Dune size could provide a possible explanation for why the two models behaved so differently at CC but similarly at AA. A simple calculation using BMAP revealed that the pre-storm CC dune had nearly 30 % less volume than the pre-storm

AA dune. This idea was tested by increasing the height of the profile between the toe and heel of the dune first by 0.25 m and then by 0.75 m. Results showed that as the dune increased in size, the predictions made by the two models began to appear more similar. Results of this comparison are provided in Appendix A.

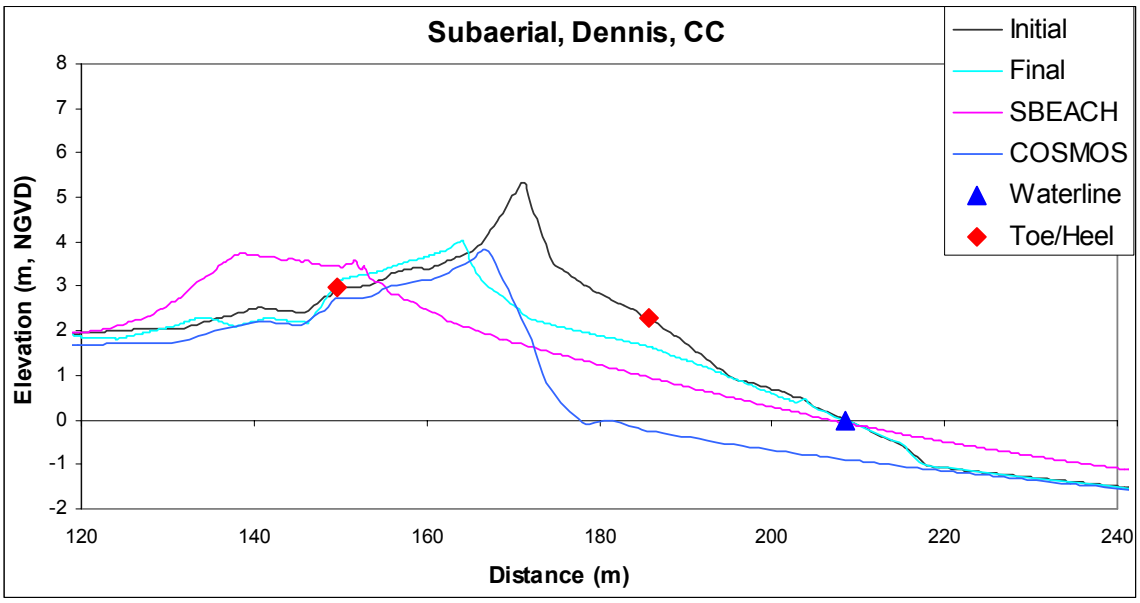

Figure 12.2. Effects of Hurricane Dennis on transect CC.

12.1.3 Transect LL

Transect LL was located nearly 1700 m south of transect AA (Overton and Fisher, 2000). The dune at this location was of comparable size to the dune at AA, about 12 % smaller in volume. Again it is not certain whether this transect was altered by maintenance before the post-storm data was collected, so quantitative analyses using the measured post-storm profile was not preformed.

Visually the two models made similar predictions as to the change in post-storm dune shape. BMAP revealed that the models made similar estimates of percent volume removed by Hurricane Dennis, 26 % by SBEACH and 31 % by COSMOS. A 28 m waterline recession was predicted by COSMOS, while SBEACH predicted 5 m

of waterline accretion. No movement of the waterline after the storm was measured, meaning the SBEACH prediction was reasonable and the COSMOS prediction was unreasonable.

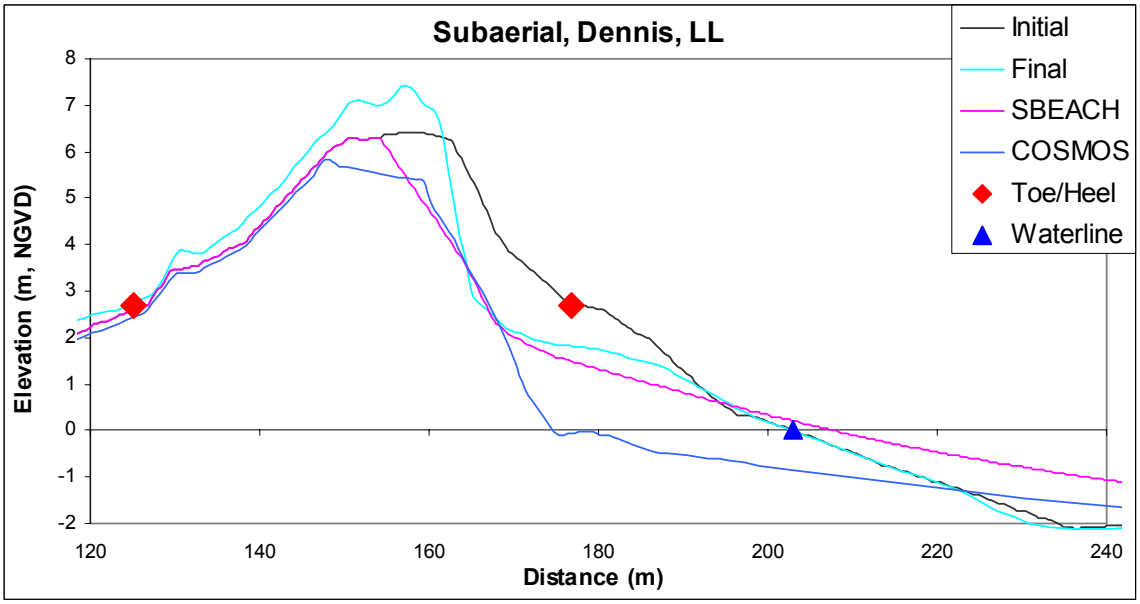

Figure 12.3. Effects of Hurricane Dennis on transect LL.

12.2 Duck, the FRF Site

Profiles 58, 62, 188, and 190 were initially selected to be used in this study because they are the furthest up-drift or down-drift of the FRF pier therefore reducing the potential influence of the pier itself as a littoral barrier. For Hurricane Isabel FRF lines 166, 174, and 176 were also selected to be evaluated. However, lines 62, 166, 176,188, and 190 did not revealed enough erosion, from either event, to be included in the Results chapter.

12.2.1 Hurricane Dennis and the FRF

After an extended stay off the North Carolina coast and essentially two land falls, Hurricane Dennis caused little subaerial change to the FRF profiles. Transects 58, 62, and 188 showed some erosion at the beach face or at the toe of the dune but little if any erosion occurred on the dunes themselves. Of the four FRF lines used to model the effects of Hurricane Dennis at the FRF, line 58 displayed the greatest amount of subaerial change and is the only case presented in this section. Figure 12.4 shows the pre and post-storm profiles as well as both model predictions for line 58. Erosion occurred mainly at the berm of the profile.

Table 12.3 displays the results for this profile. The volume considered underneath each curve is that between the point labeled Data Intersection and the waterline. Again, the Data Intersection point is where the pre-storm profile data derived from the FRF site begins, and the data from the 1998 DTM ends. In Table 13.3 the Data Intersection point is referred to as landside, meaning the landside boundary of the subaerial region being looked at.

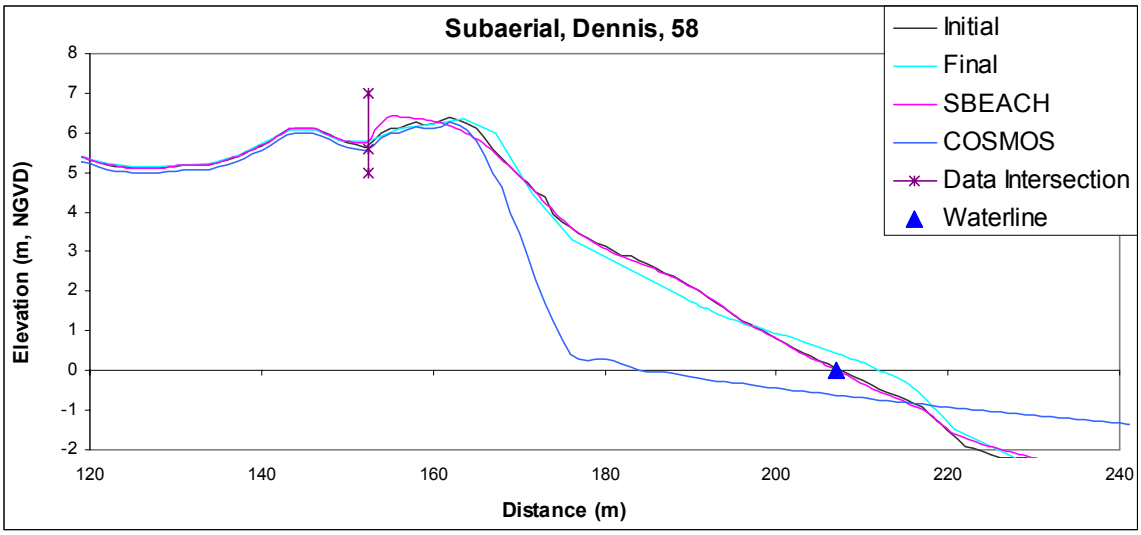

Figure 12.4. Effects of Hurricane Dennis on line 58.

Table 12.3. Profile results, FRF line 58, Hurricane Dennis.

Profile Name	Landside (m)	Waterline (m)	Volume (cu. m/m)	Percent Volume Change	Waterline Location (m)	Waterline Recession (m)
Initial (58)	152	208	188	0	208	0
Final (58)	152	208	185	2	212	5
SBEACH(58)	152	208	187	0	207	-1
COSMOS(58)	152	208	112	40	184	-24

The measured volume change between the initial and final profiles was 2 %. The SBEACH results produced a good match with the measured results. The COSMOS model performance was poor, over predicting the volume eroded subaerially by 38 %. SBEACH produced a reasonable estimate of the change in location of the waterline, while the COSMOS prediction was unreasonable, being in excess of 20 m from the measured value.

12.2.2 Hurricane Isabel and the FRF

During the course of this study Hurricane Isabel struck the Outer Banks just south of Cape Hatteras. According to the FRF, Isabel is regarded as the most significant event in their 27 year history, producing the highest waves ever recorded

at that site (FRF website, 2004). Soon after the event, wave and water level information as well as post-storm profiles measured at the FRF location were available for download. The effects from Isabel were slightly more visible then those of Hurricane Dennis, but again in most cases the erosion was limited to the beach face and not the dunes.

12.2.3 Line 58, Isabel

FRF survey line 58 again displayed the most significant erosion of all the surveyed lines examined for this storm. Figure 12.5 shows the change in the subaerial portion of line 58 as well as the predicted change from both the COSMOS and SBEACH models. The initial profile reveals a distinct berm extending almost to the waterline which is not present in the post-storm profile. This berm feature was found on several of the pre-Dennis profiles on the north end of the FRF property. Table 12.4 displays the measured and predicted percent volume change and contour recession. The total volume change between pre and post-storm surveys was measured to be 16 %. The SBEACH model prediction of 16 % and the COSMOS prediction of 21 % were both rated as good. Both models also produced reasonable estimates of the post-storm waterline location.

Table 12.4. Profile results, FRF line 58, Hurricane Isabel.

Profile Name	Landside (m)	Waterline (m)	Volume (cu. m/m)	Percent Volume Change	Waterline Location (m)	Waterline Recession (m)
Initial (58)	152.4	197	144	0	197	0
Final (58)	152.4	197	121	16	217	19
SBEACH (58)	152.4	197	122	16	203	6
COSMOS (58)	152.4	197	114	21	199	2

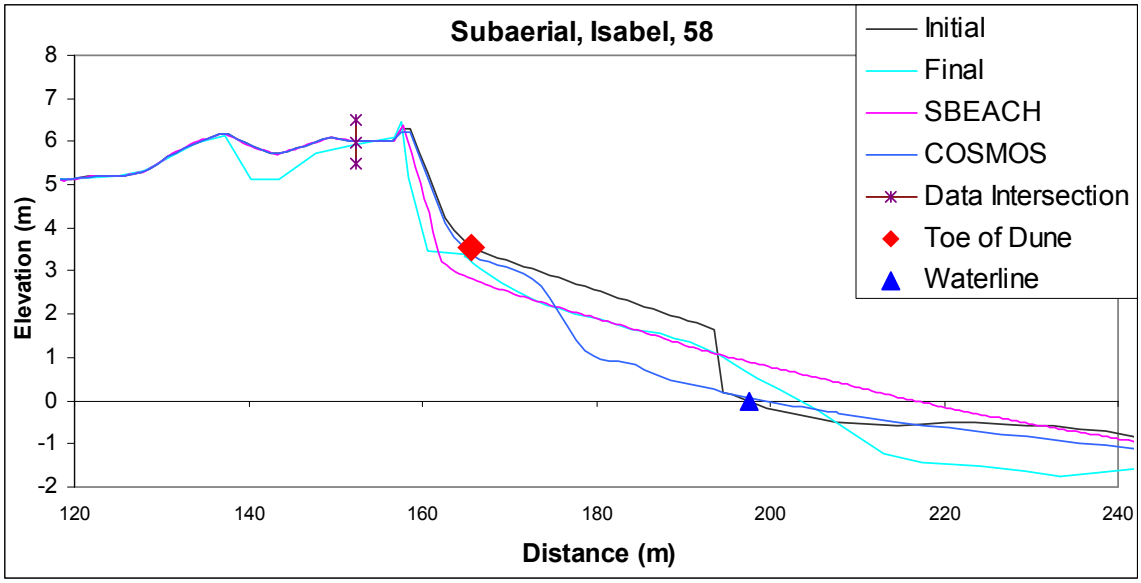

Figure 12.5. Effects of Hurricane Isabel on line 58.

Table 12.5. Dune results, FRF line 58, Hurricane Isabel.

Profile Name	Heel(m)	Toe(m)	Volume (cu. m/m)	Percent Volume Change
Initial (58)	152	166	24	0
Final (58)	152	166	17	29
SBEACH (58)	152	166	19	21
COSMOS (58)	152	166	23	4

Since Figure 12.5 indicated that erosion of the dune occurred as a result of the storm, further analysis of this profile was made focusing on the dune. The values in Table 12.5 are measured above the dune toe elevation, 3.5 m, and between the Data Intersection point and the toe of the dune. The SBEACH model received a rating of good in replicating the amount of erosion which was measured on the dune while the COSMOS model received a rating of fair.

12.2.4 Line 174, Isabel

FRF line 174, located south of the pier, also exhibited measurable erosion primarily on the beach face as shown in Figure 12.6. Table 12.6 displays the percent volume change and the waterline recession at this profile. Erosion was measured

above and landward of the waterline to the vertical line marking the Data Intersection point. Figure 12.6 shows that COSMOS predicted that Isabel would have no effect on the upper portion of the subaerial profile, but erosion would occur on the beach face. SBEACH estimated a smoothing of the upper portion and not as much erosion as estimated by COSMOS on the lower portion. Overall, within the boundaries specified, both models received a rating of good on the estimate of volume removed subaerially. Both models were also reasonably accurate in their waterline prediction.

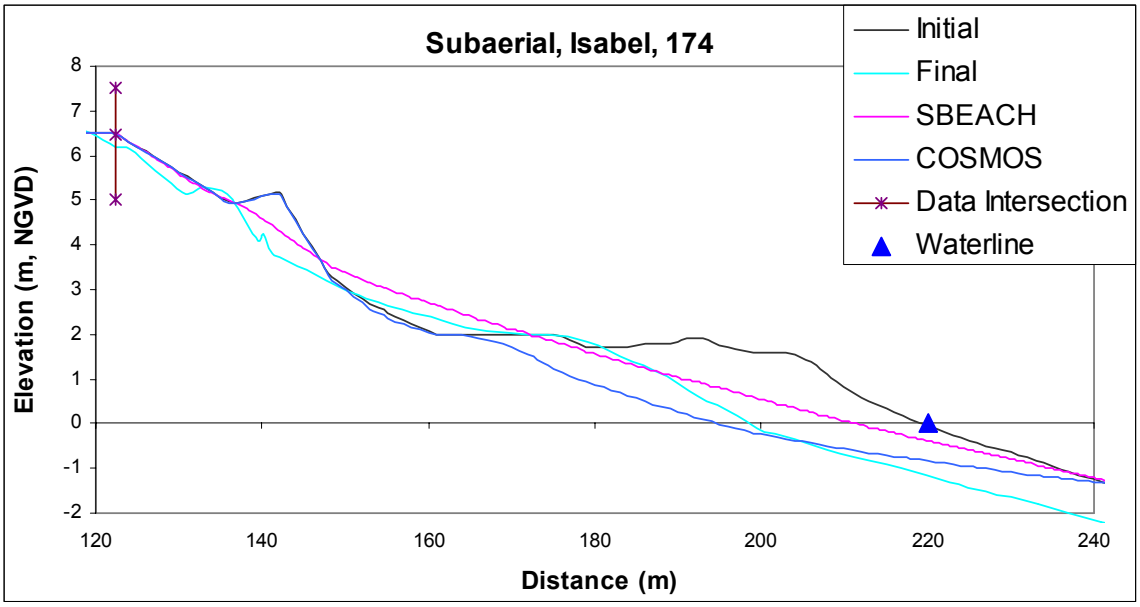

Figure 12.6. Effects of Hurricane Isabel on line 174.

Table 12.6. Profile results, FRF line 174, Hurricane Isabel.

Profile Name	Landside (m)	Waterline (m)	Volume (cu. m/m)	Percent Volume Change	Waterline Location (m)	Waterline Recession (m)
Initial (174)	122	220	256	0	220	0
Final (174)	122	220	213	17	199	-21
SBEACH (174)	122	220	233	9	211	-9
COSMOS (174)	122	220	202	21	195	-25

13. DISCUSSION

The purpose of this research was to evaluate two different numerical models as to their ability to accurately predict subaerial profile change from a given storm event. The models evaluated were individually calibrated to each study site then simulations were preformed. Results were displayed visually by plotting the pre and post-storm measured profiles as well as the predicted post-storm profile from each model. BMAP was used to calculate subaerial volumes from each profile within specified boundaries as well as to track waterline recession. A rating of good, fair, or poor was assigned to each model based on how accurately they were able to predict the subaerial percent volume change between the initial and final profile. A rating of reasonable or unreasonable was assigned to each model based on how closely they estimated the post-storm waterline location relative to the measured location.

Table 13.1. Tabulation of Rating Results.

Profile	% Volume Change Rating		Waterline Rating	
	SBEACH	COSMOS	SBEACH	COSMOS
AA - Dennis	Good	Good	Reasonable	Unreasonable
AA - Dennis (Dune)	Good	Good	Reasonable	Unreasonable
CC - Dennis	n/a	n/a	Reasonable	Unreasonable
LL - Dennis	n/a	n/a	Reasonable	Unreasonable
58 - Dennis	Good	Poor	Reasonable	Unreasonable
58 - Isabel	Good	Good	Reasonable	Unreasonable
58 - Isabel (Dune)	Good	Fair	Reasonable	Reasonable
174 - Isabel	Good	Good	Reasonable	Reasonable

Table 13.1 presents the ratings assigned to both SBEACH and COSMOS for each of the cases presented in the Results chapter. The results show that for these cases the SBEACH model performs equally as well or better than the COSMOS model as far as ability to accurately estimate percent volume change from defined

subaerial regions as well as more closely estimate the post-storm location of the waterline relative to its measured location.

In each of the profiles presented, COSMOS predicted more erosion on the beach face than did the SBEACH model. Attempts to reduce the amount of beach face erosion predicted by COSMOS through calibration were unsuccessful. Adjustment of the wave angle (Appendix C) or grain size (Appendix B) also did not improve this aspect of the COSMOS results. SBEACH on the other hand predicted only small amounts of change at the beach face in the cases provided. In several instances (line 58 for Isabel, transect LL and transect AA) SBEACH predicted the waterline to accrete. Percent changes predicted by the two models within dune regions were more similar than when analysis included the beach face.

Wave angle is a factor that was not closely looked at during this study, however, it may have deserved more consideration. As discussed in section 7.4, wave angles were not included due to a lack of available data. Not accurately accounting for the correct wave angle of incidence could have put the COSMOS model at a disadvantage since wave angle appears to play a relatively more significant role in the COSMOS model than the SBEACH model. Appendix C is provided to compare the degree to which wave angle plays a role in each model. In the case presented, a 20 degree wave angle resulted in a 16 % reduction in the amount of subaerial erosion predicted by the COSMOS model. The same wave angle yielded only a 1 % reduction in subaerial erosion predicted by the SBEACH model.

Uncertainties associated with the selection of grain size are a potential source for a variation in results from both models. The grain size variation at the FRF site

has been mentioned several times in this report. Appendix B demonstrates the sensitivity of both models to this parameter. The sediment data was downloaded from the FRF website and was used to determine a representative grain size to be used in model simulations. This data however was collected 15 years before either event took place. The value determined from that data produced mostly good results from both models for simulations of Hurricane Isabel. However, using that value at the same location (FRF line 58), to simulate Hurricane Dennis produced poor results by both models. The discrepancy is used to emphasize that accurate grain size information, collected preferably at or around the time of the modeled event, is important to reduce uncertainties associated with grain size.

The ability of both SBEACH and COSMOS to predict results that closely resemble what was measured appeared to be related to the volume of material eroded by the storm. Table 13.2 lists the volume change measured, the percent volume change measured and predicted, and the differential for each model. The profiles in bold were where the largest amounts of erosion were measured. Both models were rated as good in each of these cases and the differential for the SBEACH model decreased as volume change increased. COSMOS results were either fair or poor when the volume change was less than $43\,m^3$. At or above that value the COSMOS performance was rated as good. For both models, performance was generally better when the measured change was relatively large.

Table 13.2. Summary of Quantitative Results.

Profile	Volume Change (cu. m/m)	% Volume Change			Differential	
		Measured	SBEACH	COSMOS	SBEACH	COSMOS
AA - Dennis	65	26	22	41	4	15
AA - Dennis (Dune)	48	38	32	42	6	4
CC - Dennis	n/a	n/a	n/a	n/a	n/a	n/a
LL - Dennis	n/a	n/a	n/a	n/a	n/a	n/a
58 - Dennis	3	2	0	40	2	38
58 - Isabel	23	16	16	21	0	5
58 - Isabel (Dune)	7	29	21	4	8	25
174 - Isabel	43	17	9	21	8	4

A key difference between the two models used here is in their approach to modeling sediment transport. In the COSMOS model, sediment transport rates are mainly a function of mean velocity currents which are predicted from wave parameters. The SBEACH model places less emphasis on process description by directly relating sediment transport rates to wave parameters. While it is a less sophisticated design it produced better results with given data.

Roelvink and Broker (1993) evaluated five process-based cross-shore numerical models (COSMOS being one of them) in a paper titled "Cross-shore Profile Models". In their conclusion section they state, describing the group of models as a whole, "at present it is clear that all errors in every step in the morphological calculations are not only added up but may influence the successive calculations in a wrong direction". For example, if in the COSMOS model, a poor prediction of current velocity is made, then the estimated sediment transport rates will suffer.

Though replicating the physical processes may make COSMOS more prone to errors, relying on empirical data may reduce SBEACH's applicability. SBEACH was developed using data from wave tank tests and then verified using field data from a number of east coast sites including the FRF. For the study sites used here, this probably gives SBEACH an advantage over the COSMOS model whose field verification included data from a broader range of geographic locations. Using field data from a variety of locations to compare SBEACH and COSMOS may have provided for a more comprehensive comparison.

In a study conducted by Komar *et al.* (1999) on the Oregon coast of the U.S. both SBEACH and COSMOS were used along with a geometric model to identify a range of potential foreshore and dune erosion cases resulting from extreme conditions. The beaches along the Oregon coast are described as dissipative; having very gentle slopes causing waves to break far offshore. The beach at the FRF site may be categorized as a reflective beach because the slopes on the foreshore are generally steep, and waves tend to break right on the beach itself (Larson and Kraus, 1989).

The results from the geometric model were used as the maximum likely erosion, and SBEACH and COSMOS were used to indicate the minimum likely erosion. The two numerical models were expected to under predict erosion because of their inability to account for infragravity motions in the surf zone (Komar *et al*., 1999). In Komar's results, for the 50 year event, the geometric model predicted a waterline retreat of 87 m, while COSMOS and SBEACH predicted a retreat of 27 and 10 m respectively.

Consistent with what has been seen in the present work, Komar also finds the COSMOS model to predict greater waterline recession than SBEACH. Inconsistent with this work is that Komar states in the article by Komar *et al*. (1999) that the COSMOS result is expected to be the more reliable indicator. This discrepancy is a good example of how COMOS maybe more appropriately applied to a different situation.

13.1 Conclusion

The SBEACH model produced good results in all cases analyzed; COSMOS produced good results in cases where more than $40\,m^3$ of volume was removed between the defined boundaries. Prediction of waterline recession was reasonable in all cases using the SBEACH model, but unreasonable in all but two cases using COSMOS. COSMOS consistently over predicted the amount of erosion on the beach face.

Despite the evidence presented here that the SBEACH model consistently performs equally as well or better than the COSMOS model, it seems that nearshore models are becoming more process based. Research in coastal processes is ongoing and our understanding of the environment is maturing. As such our ability to replicate the physical processes will continue to improve and process-based models such as COSMOS will become more accurate. Schooneees and Theron (1993), in their assessment of 10 cross-shore models touch on the development potential of the more theoretical models, like COSMOS. They make the point that such models are better equipped to incorporate new processes as well as improve those processes already established, giving them the ability to be more widely applicable than the

empirical models. They also make the point, however, that there is a danger associated with including more and more processes. That as processes become too specific the model may become overly sensitive to input parameters.

In the current state of development of these two models, the SBEACH model is the preferred model by the author. SBEACH produced good results in the cases analyzed. The COSMOS model predicted good or fair results within the dune region, but consistently over predicted erosion on the beach face and recession of the waterline. However, using data from a variety of locations, instead of two that are geographically similar, might have provided examples where the COSMOS model performed better. The data used here was what was available to the author, and it is felt that the evidence provided here may be a useful indicator of the strengths of both SBEACH and COSMOS in terms of overall results.

14. REFERENCES

Bailard, J. A. 1981. An Energetics Total Load Sediment Transport Model for a Plane Sloping Beach. Journal of Geophysical Research, vol. 86, pp.10,938-10,954.

Barnes, J. 2001. North Carolina's Hurricane History, 3rd edition. The University of North Carolina Press. Chapel Hill & London.

Bosboom, J. 2000. Wind-Wave Induced Oscillatory Velocities Predicted by Boussinesq Models. Terra et Aqua, no. 80.

Dally, W. R., Dean, R. G. and Dalymple, R. A. 1985. Wave Height Variation Across Beaches of Arbitrary Profile. Journal of Geophysical Research, vol. 90, no. C6, pp.11917-11927

Dean, R. G., Dalymple, R. A. 1984. Water Wave Mechanics for Engineers and Scientists. Prentice-Hall, Inc. Englewood Cliffs, New Jersey.

Grasmeijer, B. T. and Ruessink, B. G. 2003. Modeling of waves and currents in the nearshore parametric vs. probabilistic approach. Coastal Engineering, vol. 49. pp. 185-207

Komar, P. D., McDougal, W. G., Marra, J. J. and Ruggiero, P. 1999. The Rational Analysis of Setback Distances: Applications to the Oregon Coast. Shore & Beach, vol. 67, no. 1, pp. 41-49.

Larson, M. (1995). Model for decay of random waves in the surf zone. Journal of Waterways, Port, and Coastal Engineering, vol. 121, pages 1-12.

Larson, M. and Kraus, N. C. 1989. SBEACH: Numerical model for simulating Storm-induced beach change. Report 1: Empirical foundation and model development, technical report CERC-89-9. Coastal Engineering Research Center. Vicksburg, MS: U.S. Army Corps of Engineers, Waterways Experiment Station.

Larson, M., Kraus, N. C. and Byrnes, M. 1990. SBEACH: Numerical model for simulating Storm-induced beach change. Report 2: Numerical foundation and model development, technical report CERC-89-9. Coastal Engineering Research Center. Vicksburg, MS: U.S. Army Corps of Engineers, Waterways Experiment Station.

Miller, P. R. 1998. Evaluating Existing Cross-Shore Sediment Transport Models for a Steep, Porous Beach; Waimea Bay Beach, O'ahu, Hawaii. Masters Thesis, Department of Ocean Engineering of the University of Hawaii.

Nairn, R. B. and Southgate, H. N. 1993. Deterministic profile modeling of nearshore processes. Part 2. Sediment transport and beach profile development. Coastal Engineering, vol. 19, pp. 57-96.

National Weather Service website (2004).
http://www.erh.noaa.gov/er/akq/wx_events/hur/isabel_2003.htm

NOAA Website (2004). http://www.co-ops.nos.noaa.gov/benchmarks/

Overton, M. F. and Fisher, J. S. 2000. NC12 Vulnerability Analysis. Department of Civil, Construction and Environmental Engineering, North Carolina State University.

Overton, M. F. and Fisher, J. S. 2003. The 1998 Long-term Erosion Rate Update Study for the North Carolina Shoreline. Civil, Construction and Environmental Engineering, North Carolina State University.

Overton, M. F. and Fisher, J. S. 2004. The 1998 Long-term Erosion Rate Update: Methods Report. Civil, Construction and Environmental Engineering, North Carolina State University.

Roelvink, J. A. and Broker, I. 1993. Cross-shore profile models. Coastal Engineering, vol. 21, pp.163-191.

Rosati, J. D., Wise, R. A., Kraus, N. C. and Larson, M. 1993. SBEACH: Numerical model for simulating storm-induced beach change. Report 3: User's Manual, technical report CERC-89-9. Coastal Engineering Research Center. Vicksburg, MS: U.S. Army Corps of Engineers, Waterways Experiment Station

Schjoonees, J. S. and Theron, A. K. 1995. Evaluation of 10 cross-shore sediment transport/morphological models. Coastal Engineering, vol. 25, pp. 1-41.

Southgate, H. N., 1989. A nearshore profile model of wave and tidal current interaction. Coastal Engineering, vol. 13, pp. 219-245.

Southgate, H. N. and Nairn, R. B., 1993. Deterministic profile modeling of nearshore processes. Part 1. Waves and currents. Coastal Engineering, vol. 19, pp. 27-56

Wise, R. A., Smith S. J. and Larson, M. 1996. SBEACH: Numerical model for simulating Storm-induced beach change. Report 4: Cross-shore transport under random waves and model verification with Supertank and field data, technical report CERC-89-9. Coastal Engineering Research Center. Vicksburg, MS: U.S. Army Corps of Engineers, Waterways Experiment Station.

U.S Army Corps of Engineers Field Research Facility Website (2004).
http://www.frf.usace.army.mil/

Veri Tech Website (2004).
http://www.veritechinc.com/navigate.htm

APPENDIX A

Effects of Increasing Dune Height at Buxton
Transect CC.

Results indicate that as the dune height was increased, the model predications became more similar. Figure A1 shows model results when the actual dune size was used. Figure A2 shows the model results when the initial dune height at transect CC was increased by 0.25 meters between the toe and heel of the dune. Figure A3 shows model results when the dune height was increased by 0.75 meters. Table A1 displays the predicted post-storm dune volumes remaining by both SBEACH and COSMOS for each of the three scenarios. As indicated by the figures, the volume remaining within the dune that is predicted by the two models becomes more similar as the dune gets bigger.

Table A1. Comparison of model predictions as dune size was increased.

Dune CC	Dune Volume Remaining (cu. m/m)	
	SBEACH	COSMOS
Normal	8	17
0.25 m Increase	18	22
0.75 m Increase	35	36

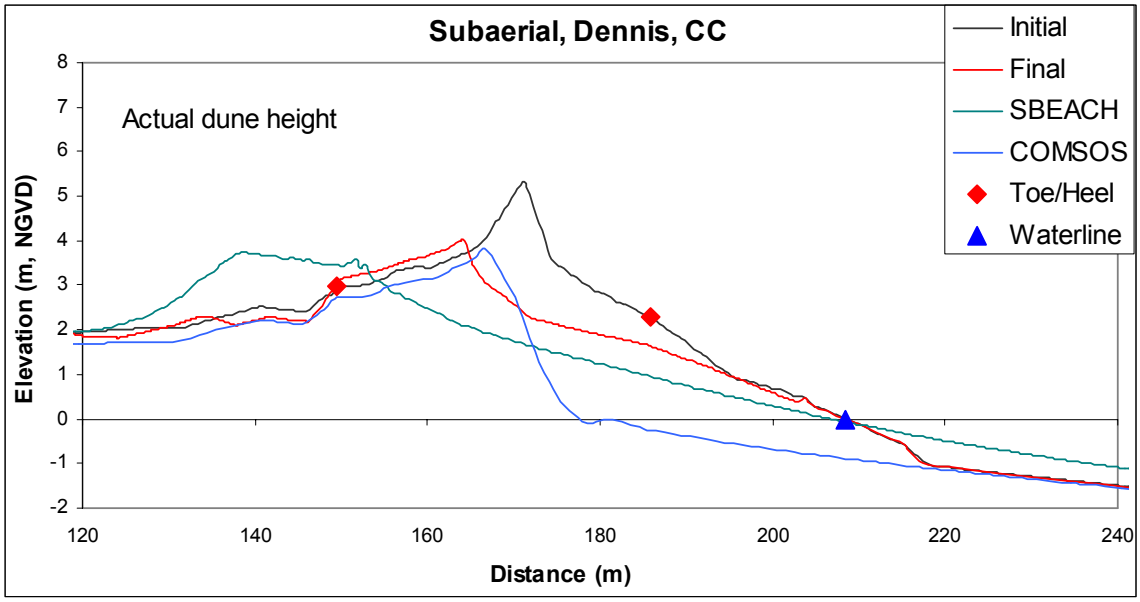

Figure A1. Using actual CC dune size.

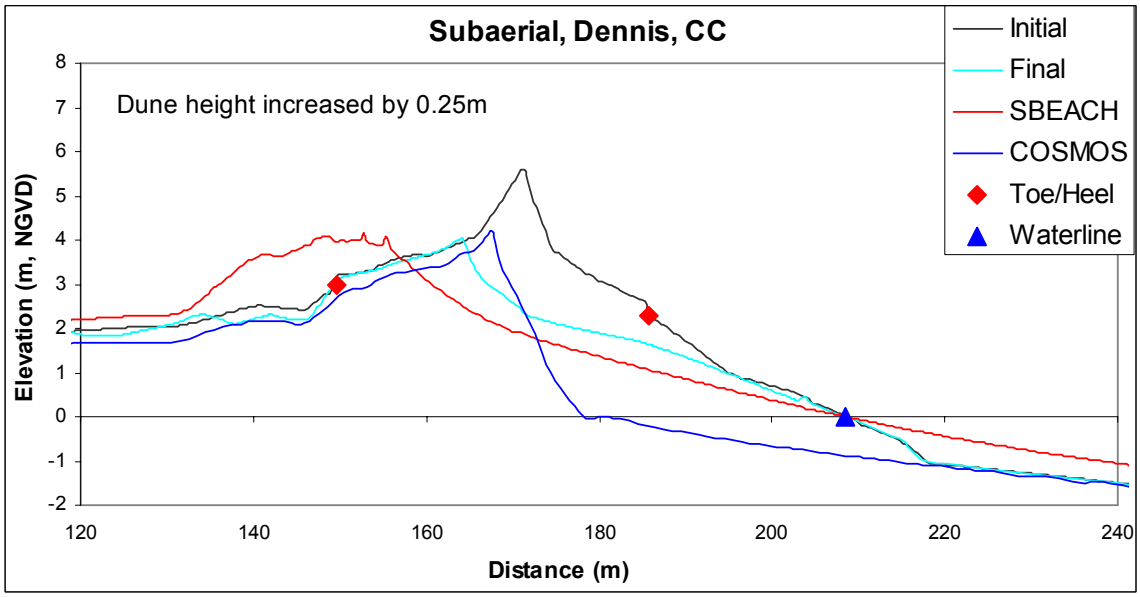

Figure A2. CC dune increased by 0.25 m.

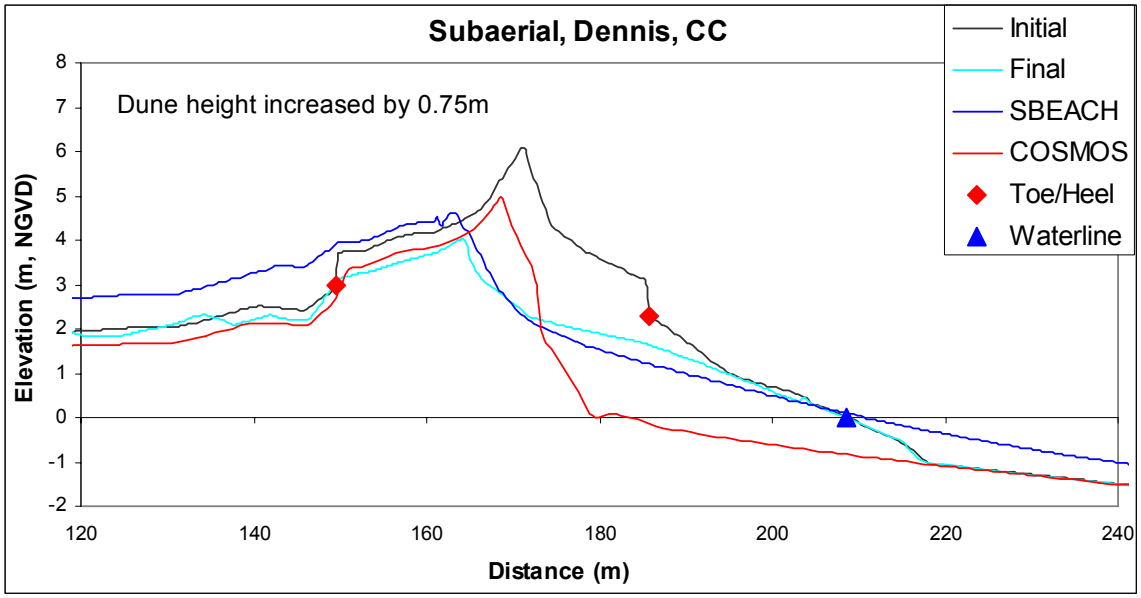

Figure A3. CC dune increased by 0.75 m.

APPENDIX B

FRF Grain Size Determination for Hurricane Dennis Simulations.

Both models, when using the grain size values determined by the process laid out in section 9.2 produced mostly good or fair results for simulations of Hurricane Isabel at the FRF location. Both models, however, produced poor results for simulations of Hurricane Dennis. Investigation into the effect of adjusting the grain size parameter was preformed using FRF line 58.

The measured volume change after Hurricane Dennis at line 58 between the Data Intersection point and the waterline was just 2 %. The measured waterline recession after Hurricane Dennis was 5 m. Table B1 displays the results from both models as the representative grain size for FRF line 58 was incrementally increased from 0.42 mm, the value determined for that profile using the samples collected during March 1984 through September 1985.

Table B1. Model results as a function of grain size.

	Percent Volume Change		Waterline Recession	
Grain Sizes(mm)	SBEACH	COSMOS	SBEACH	COSMOS
0.42	44	58	-6	-29
0.50	34	52	-4	-27
0.60	18	48	-1	-26
0.70	5	44	0	-24
0.80	0	40	0	-23
0.90	0	37	1	-21

Both models over estimated the percent volume change resulting from Dennis when using a mean sediment size of 0.42 mm. When the value was increased to 0.50 mm a 10 % reduction in the predicted volume change by SBEACH resulted, while a 6 % reduction was seen in the COSMOS results. Increasing the mean grain size to 0.60 mm resulted in a 26 % change in SBEACH while only a 10% change in COSMOS. With a value of 0.70 mm the SBEACH results fell within the good range while the COSMOS model results were still poor. Increasing the grain size to 0.80 mm resulted

in a zero percent volume change estimated by SBEACH, but a 40 % volume change in COSMOS. The author decided to use 0.80 mm as the assumed representative grain size value at the FRF for simulations of Hurricane Dennis.

These results indicate the SBEACH is more sensitive to mean grain size than COSMOS. In order to produce a 10 % change in model results for the prediction of percent volume change, the grain size was increased by 44 % in COSMOS (0.42 mm to 0.60 mm). SBEACH required only a 20 % increase in grain size (0.42 mm to 0.50 mm) to achieve a 10 % change in results.

Figures B1 and B2 are provided to illustrate how model results changed as a result of increasing the grain size.

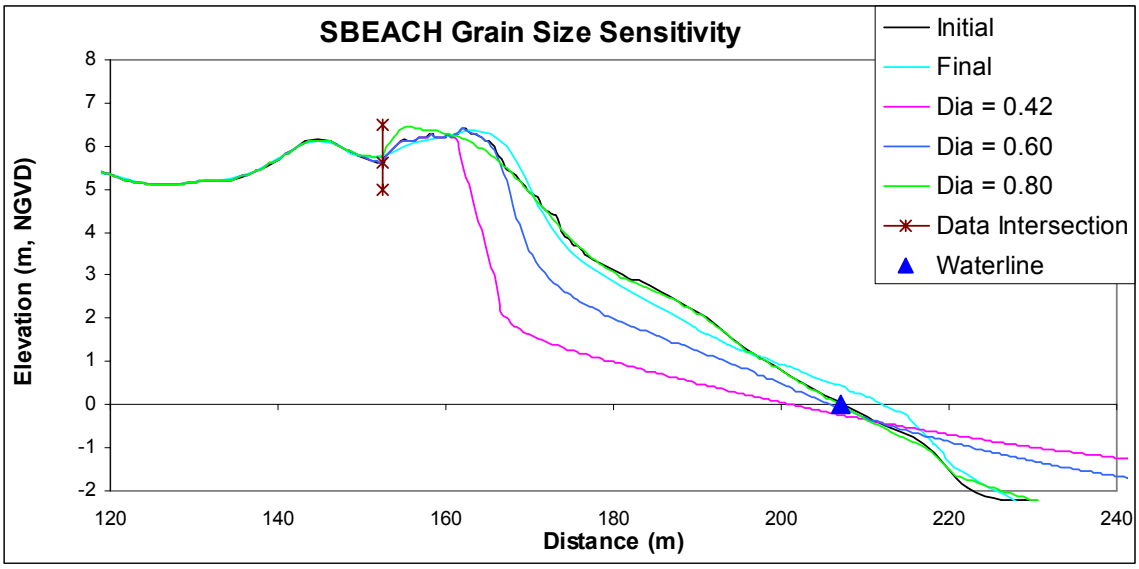

Figure B1. FRF transect 58, Hurricane Dennis, using SBEACH

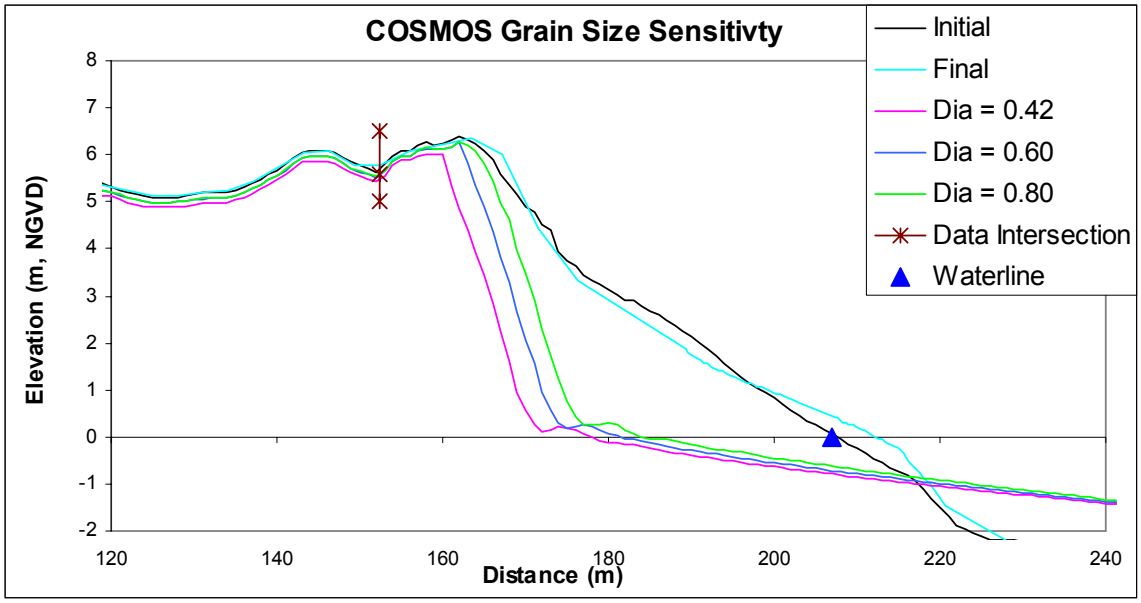

Figure B2. FRF transect 58, Hurricane Dennis, using COCMOS.

APPENDIX C

Sensitivity to Wave Angle.

Incident wave angle is the angle between bathymetric contours and the wave crest. When a wave approaches the beach at an angle, refraction occurs reducing both the energy and height of the wave. Wave refraction is accounted for in both models by applying Snell's law. Figures C1 and C2 illustrate the degree to which the effects of refraction influence model prediction. An angle of incidence is required by both models before a simulation can be initiated. The angle of incidence is measured relative to how far it deviates from 90 degrees to the shoreline. When waves approach the shore at 90 degrees they are said to be normally incident, for such a case the angle of incidence is given a value of zero.

By visually comparing Figure C1 and C2, it appears that COSMOS is more sensitive to variation in wave angle. Table C1 quantifies this by displaying percent volume change and waterline recession values for various angles of incidence relative to using normally incident wave angles. The difference between the two models may be attributed to the fact that the wave model used in COSMOS includes interaction between waves and longshore currents. Even though the version of COSMOS used in this comparison is only a two dimensional model, effects from longshore currents are still accounted for through refraction and a wave friction factor (Southgate and Nairn, 1993). While the SBEACH model focuses only on transport perpendicular to the coast. The SBEACH literature recommends that a wave angle of zero be used unless the incident angles are highly oblique (Rosati *et al.*, 1993).

Table C1. Effects of using obliquely incident waves.
Values are relative to those produced using normally incident waves.

Wave Angle (degrees)	Percent Volume Change		Waterline Recession (m)	
	SBEACH	COSMOS	SBEACH	COSMOS
10	0	5	0	2
20	1	16	0	6
45	4	27	0	8

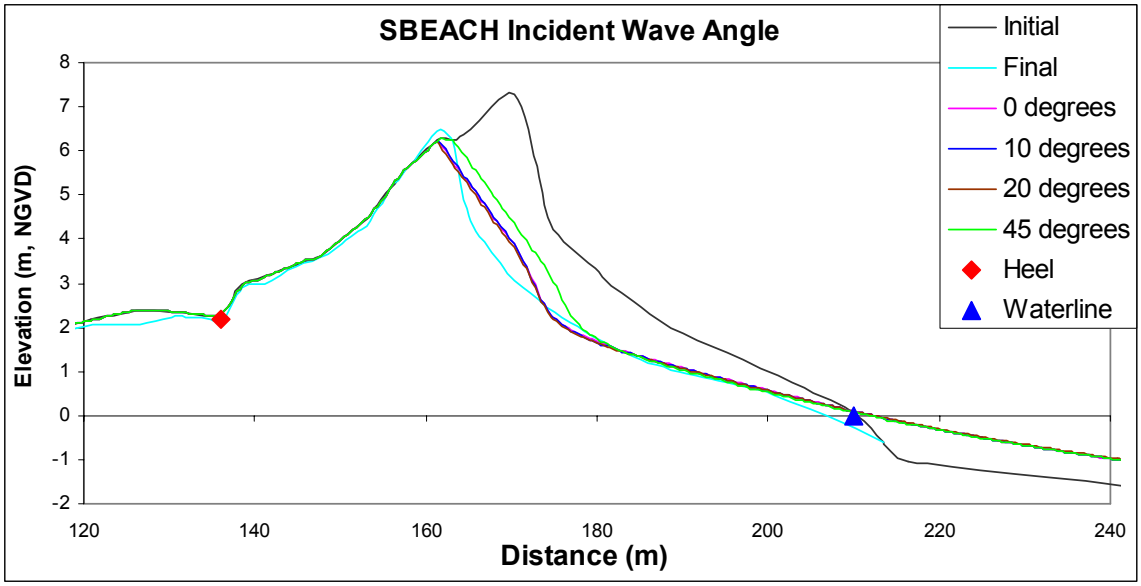

Figure C1. The effect of wave angle variation using SBEACH.

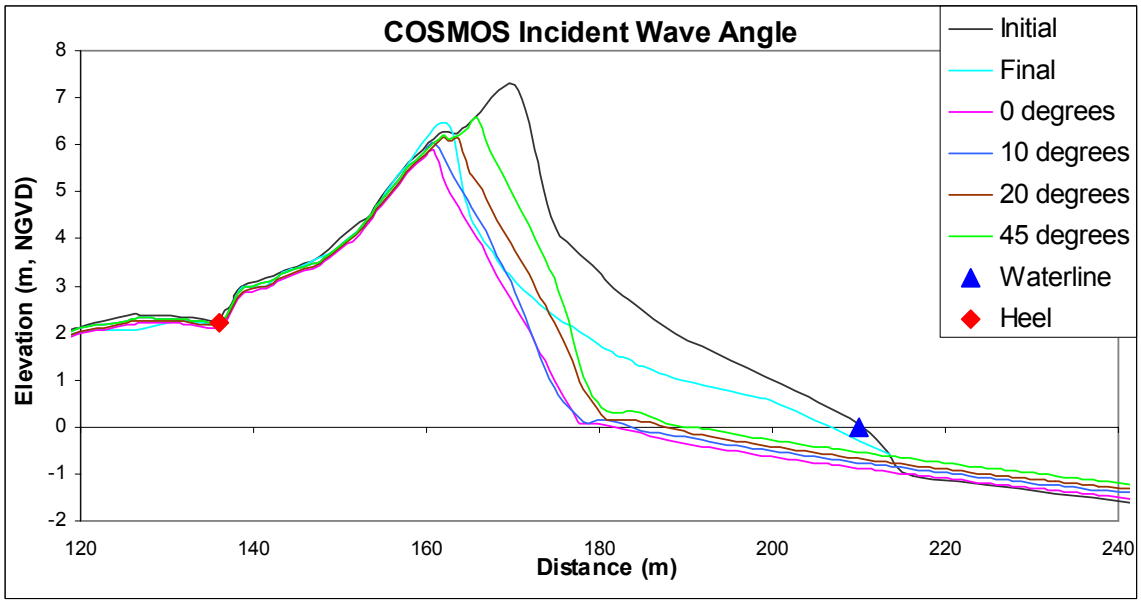

Figure C2. The effect of wave angle variation using COSMOS.

APPENDIX D

Estimation of the Maximum Horizontal Fluctuation of the Waterline Location due to Tidal Cycles.

The tidal range (MLLW to MHHW) at the FRF pier and at the Cape Hatteras fishing pier, according to the 1983 – 2001 epoch, are 1.124 m and 1.056 m respectively (NOAA website, 2004). These values were used to estimate the maximum daily horizontal variation of waterline location at the FRF and at Buxton. The beach slope, between the dune toe and waterline, was estimated from a profile from each site, AA for the Buxton site and line 58 for the FRF site. Using the tidal ranges, 1.124 m (FRF) and 1.056 m (Buxton), and the profile slopes, the horizontal fluctuation was estimated for each site.

For the FRF site the horizontal fluctuation due to tidal action was estimated to be 11.8 meters, and for the Buxton site it was estimated to be 9.5 meters. The average of these two values, 11 meters, was used to account for errors that may be related to data collection techniques and not model performance.